

Assessment of Biodegradation Potential of Diluted Bitumen

by

Patrick William Faught

Honors Thesis

Appalachian State University

Submitted to the Department of Chemistry  
and The Honors College  
in partial fulfillment of the requirements for the degree of

Bachelor of Science

May, 2019

Approved by:

---

Robert Swarthout, Ph.D., Thesis Director

---

Megen Culpepper, Ph.D., Second Reader

---

Cara Fiore, Ph.D., Second Reader

---

Libby Puckett, Ph.D., Departmental Honors Director

---

Jefford Vahlbusch, Ph.D., Dean, The Honors College

**Dedicated to Bill and Karla Fought**

## Table Of Contents

1. Abstract	7
2. Introduction	8
3. Methods	16
3.1. Diluted Bitumen Samples	17
3.2. Sand Microcosm Experiment	17
3.3. WAF Microcosm Experiment	18
3.4. Microcosm Extraction	20
3.5. Standard Prep	21
3.6. GC-ToF-MS Analysis	21
3.7. Data Analysis	21
3.8. QA/QC	24
3.9. Microbial Analysis	26
4. Results	27
4.1. Sand Microcosm Experiment	27
4.1.1. GC-ToF-MS Chromatogram Time Series	27
4.1.2. Biodegradation Indicators	29
4.2. WAF Microcosm Results	30
4.2.1. Oil Quantification	30
4.2.2. GC-ToF-MS Chromatogram Time Series	32
4.2.3. Biodegradation Indicators	36
5. Implications and Future Work	38
6. Conclusions	40
7. References	41

## Table of Figures

Figure 1. Depiction of various classes of hydrocarbons found in crude oil. ....	8
Figure 2. GC Comparison of alkane constituents of dilbit and Macondo well (DWH) (Swarthout et. al, 2017) .....	9
Figure 3. Aftermath of Gogoma train derailment (CBC, 2015) .....	10
Figure 4. Weathering processes of spilled oil (Stringari et al., 2013) .....	11
Figure 5. Different chemical pathways for the photochemical oxidation of naphthalene (McConkey et al., 2002) .....	13
Figure 6. Typical reactions catalyzed by hydrocarbon monooxygenases and dioxygenases (Stout, Wang, 2016) .....	15
Figure 7. Representative microcosm using sand method (nitrogen and phosphorus treatment, day 42, replicate B) .....	17
Figure 8. Sand microcosm setup and extraction. ....	18
Figure 9. Preparation of the water-accommodated fraction .....	19
Figure 10. WAF microcosm setup and extraction. ....	20
Figure 11. (A) Chemical structure of n-C <sub>17</sub> , pristane, n-C <sub>18</sub> , and phytane. (B) Extracted ion chromatogram depicting n-C <sub>17</sub> and pristane, n-C <sub>18</sub> and phytane (m/z = 57) .....	23
Figure 12. Chromatogram overlay of neat oil and day 0 sample .....	27
Figure 13. Sand microcosm experiment chromatograms comparing day 21 samples for (a) the total PAH signature (m/z = 128, 152, 153, 166, 184, 178, 202, 228, 252, 276), and (b) the alkane signature (m/z = 57) .....	28
Figure 14. Traditional indicators of alkane biodegradation for (A) n-C <sub>17</sub> /pristane and (B) n-C <sub>19</sub> /phytane ratios for dilbit samples over the course of 21 days. ....	29
Figure 15. Hopane-normalized concentrations of alkanes and PAHs in live and nutrient spiked (NP) treatments at day 21 compared to the negative control (Dead) .....	30
Figure 16. Internal Standard normalized calibration curve for triacontane .....	31
Figure 17. Neat Cold Lake dilbit sample (blue trace) and WAF sample (red trace) GC-ToF-MS total ion chromatogram. ....	32
Figure 18. Dead sample TIC chromatograms at day 0 (black) and day 21 (purple) normalized to hopane .....	33
Figure 19. Extracted ion chromatograms depicting the alkane region (m/z=57) of dead microcosms at day 0 (black) and day 21 (purple) normalized to hopane. ....	33
Figure 20 Extracted ion chromatogram of the PAH region (m/z = m/z = 128 + 152 + 153 + 166 + 184 + 178 + 202 + 228 + 252 +276) of d microcosms at day 0 (black) and day 21 (purple) normalized to hopane. ....	34

Figure 21. Live sample TIC chromatograms at day 0 (black) and day 21 (purple) normalized to hopane .	35
Figure 22. Extracted ion chromatogram of the alkane region ( $m/z = 57$ ) of live microcosms at day 0 (black) and day 21 (purple) normalized to hopane. ....	36
Figure 23. Extracted ion chromatogram of the PAH region ( $m/z = m/z = 128 + 152 + 153 + 166 + 184 + 178 + 202 + 228 + 252 + 276$ ) of live microcosms at day 0 (black) and day 21 (purple) normalized to hopane. ....	37
Figure 24. Traditional indicators of alkane biodegradation for (A) $n\text{-C}_{17}$ /pristane and (B) $n\text{-C}_{18}$ /phytane ratios for dilbit samples over the course of 21 days. ....	38
Figure 25. Hopane-normalized concentrations of alkanes and PAHs in live treatment at day 21 compared to the negative control (Dead) .....	35

## Table of Tables

Table 1. Alkane calibration standard preparation .....	21
Table 2. List of compounds in dilbit analyzed for both microcosm experiments with mass-to-charge ratios and retention times. ....	19
Table 3. Surrogate recoveries for all extracted sand microcosms (Nomenclature: d=Dead, L=live, NP = nitrogen and phosphorus, number = day extracted A-C = replicate microcosms) .....	25
Table 4. Surrogate recoveries for all extracted microcosms (WAF) .....	26
Table 5. Total peak areas for TIC, alkanes, and PAH region of dead microcosms. ....	34
Table 6. Total peak areas for TIC, alkanes, and PAH region of live microcosms .....	36

## **1. Abstract**

Diluted bitumen (dilbit) is a mixture of heavily weathered crude oil derived from oil sands and a lighter petroleum product diluent. Diluted bitumen is starting to comprise a greater proportion of oil imports to the U.S., and is the primary oil being transported by the Keystone XL Pipeline. Another common way to transport dilbit is by shipping tankers. Thus, it is critical to assess the extent of which it degrades in water. To test this, two different microcosm setups were prepared, one with autoclaved sand spiked with oil, and one with a water-accommodated fraction of oil. Three separate conditions for the water were prepared for the sand microcosm: water that has been autoclaved to kill microbes present(control), water with the natural flora present (alive), and water with natural flora and added nitrogen and phosphorus (N&P). The water-accommodated fraction microcosms utilized autoclaved water and natural seawater. At several time points, the remaining crude oil in the samples was extracted and analyzed by gas chromatography and time-of-flight mass spectrometry (GC-TOF-MS.) Results from these microcosm experiments serve as a stepping-off point for future biodegradation studies.

## 2. Introduction

Bitumen is a heavily weathered, high-sulfur, viscous source of crude oil derived from Canadian oil sands. With a viscosity of  $>10,000$  centipose<sup>1</sup>, bitumen is not viable for pipeline transport in its natural state. In order to overcome this, bitumen is diluted with natural gas condensate or other light petroleum products to the proper viscosity and density to form “dilbit.” Increased consumption of bitumen oil has spurred further extraction and transportation by pipeline, rail, and tanker. Because of this, dilbit is starting to comprise a larger proportion of oil imports to the United States in this manner, with over 230 million barrels imported in 2013 alone.<sup>2</sup>

Crude oil contains a myriad of chemical compounds which can be grouped into four main classes based on structure (Figure 1). These include alkanes (normal, branched, cyclic), polycyclic aromatic hydrocarbons (PAHs), biomarkers such as hopane, and polar compounds (resins and asphaltenes).<sup>3</sup> Dilbit contains a much greater proportion of heavier n-alkanes and PAHs compared to conventional sources of crude.

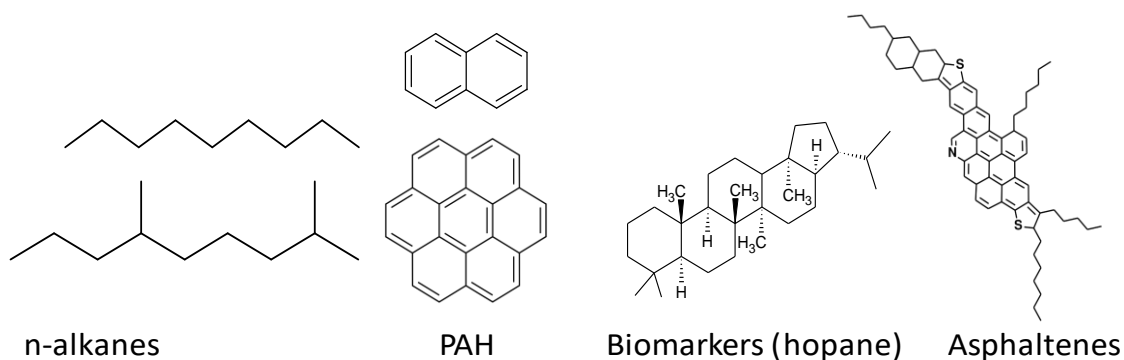


**Figure 1. Depiction of various classes of hydrocarbons found in crude oil.**

Dilbit’s viscosity can be attributed to a high abundance of resins and asphaltenes, structures that are not completely understood by scientists. Its high viscosity requires dilution for pipeline transportation. Figure 2 depicts a chromatogram comparing dilbit to a traditional light, sweet crude oil, the Macondo



well oil released during the *Deepwater Horizon* disaster. These chromatograms were generated using a gas-chromatogram coupled to a flame-ionization detector.

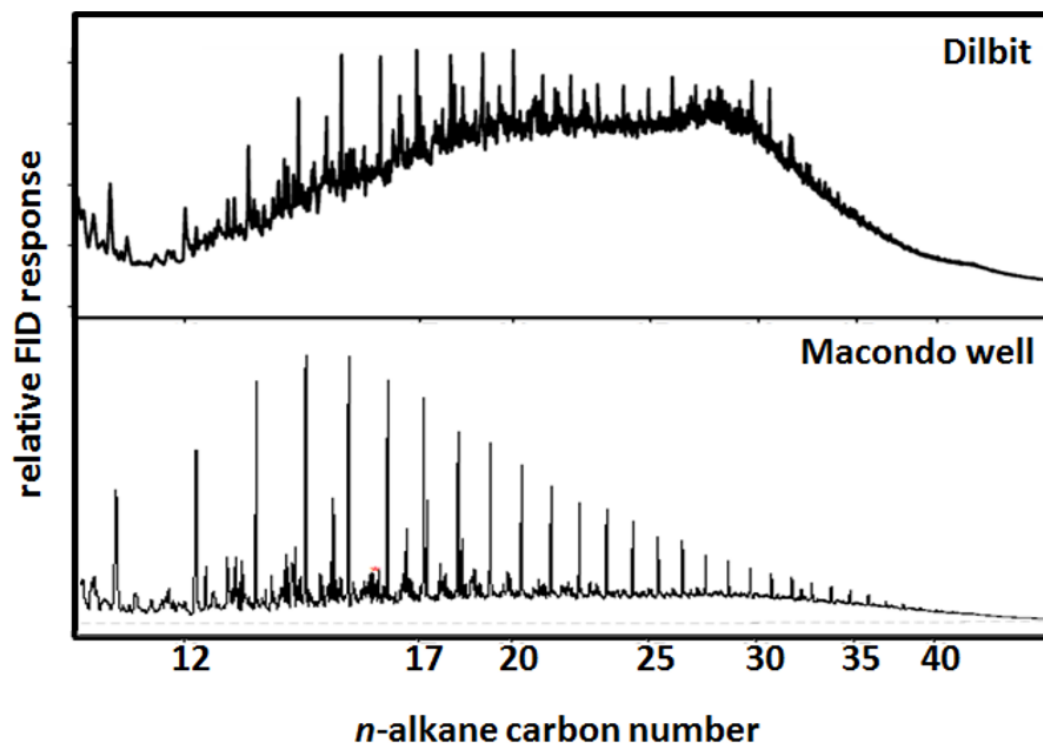


**Figure 2. GC Comparison of alkane constituents of Dilbit and Macondo well (DWH)<sup>4</sup>**

Because dilbit production is relatively new, there has been much debate on the best method for transportation with the majority of the discussion focused on rail and pipeline transport. Compared to rail transport, pipelines result in fewer greenhouse gas emissions.<sup>5</sup> However, these pipelines have less oversight, are susceptible to corrosion and are prone to land rights disagreements. The difficulty of monitoring and maintaining thousands of miles of pipeline has led to numerous spills. The first pipeline spill of diluted bitumen occurred on July 26, 2010, when a pipeline owned by Enbridge Energy Partners LLP broke and released over 800,000 gallons of dilbit into the Kalamazoo River, MI. This resulted in the costliest inland spill in US history<sup>6</sup>, affecting areas more than 25 miles downstream. This pipeline spill was twelve times more costly to clean up per-gallon than the *Deepwater Horizon* spill in 2010.<sup>4</sup>

Rail transportation allows for greater flexibility for delivery, but is more costly to operate, with the potential of derailments or collisions.<sup>7</sup> One such instance occurred on February 14, 2015, in which a Canada National (CN) train containing 29 containers of dilbit derailed near Gogama, Canada. According to CN, 15 tank cars ruptured, and released dilbit, 7 of which caught fire. According to an estimate by Canada's Transportation Safety Board, just under 700,000 gallons of dilbit was spilled, affecting nearby wetlands and streams.<sup>8</sup>



**Figure 3. Aftermath of Gogoma train derailment<sup>8</sup>**

With the proposed expansion to the Trans Mountain pipeline connecting the oil sands production region to the coastal port of Burnaby, British Columbia, transport of dilbit to coastal ports is likely to increase as Canada seeks to access overseas markets. In addition, dilbit is currently used as a fuel for ships. Given that the production of dilbit is increasing and that large-scale transport by tanker ship is likely, a future spill in a marine environment is plausible. To prepare for this inevitability it is critical to understand the environmental fate and behavior of diluted bitumen in a marine environment.

Once spilled, crude oil is exposed several concurrent physical, phase change, chemical and biological processes, collectively called oil weathering processes (OWP), which work in-tandem to change the physical and chemical properties of the spilled oil. Physical weathering processes include

spreading, dispersion into the water column, emulsification, adsorption to suspended colloidal particles, and sedimentation, while phase change, chemical and biological processes include evaporation, dissolution, photochemical oxidation and biodegradation. Most physical processes alone do not affect the chemical composition of spilled oil, however, they greatly affect the rates by which the bulk oil composition will be altered by evaporation and dissolution, and the rate at which individual oil compounds will be transformed by photochemical oxidation and biodegradation.<sup>9</sup>

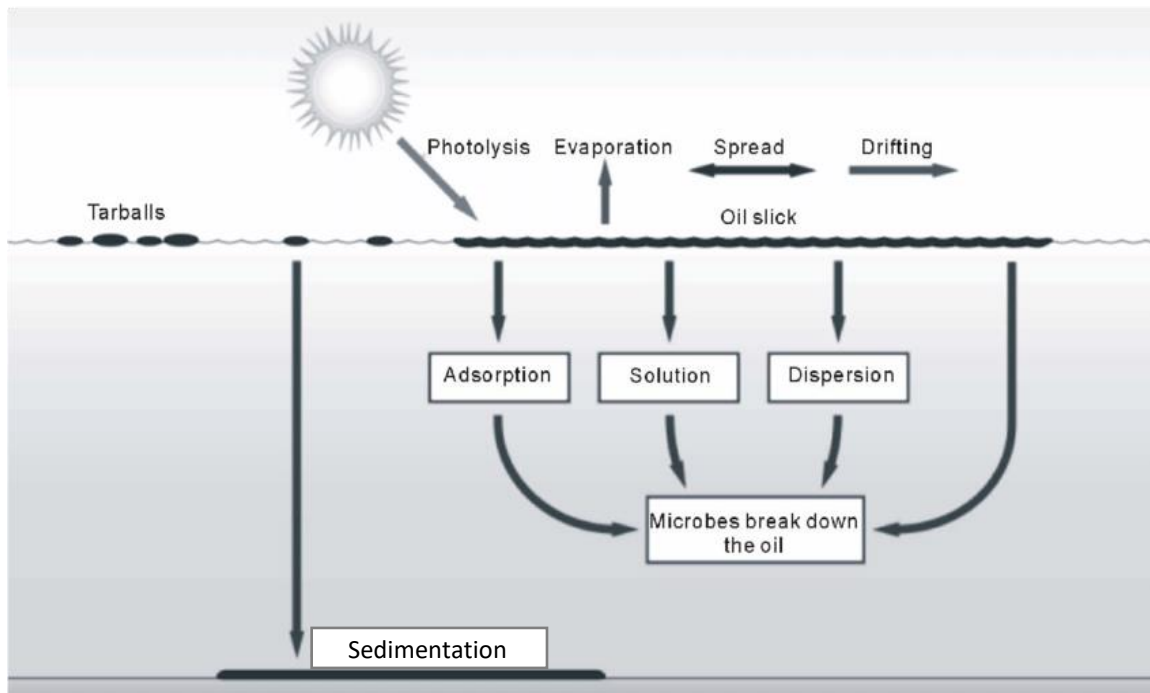


**Figure 4. Weathering processes of spilled oil<sup>10</sup>**

Observations of the fate of dilbit spilled during the 2010 Kalamazoo River spill indicated that the oil rapidly sunk to the river bottom. Prompted in part by this spill, the federal government of Canada announced the World Class Tanker Safety System in 2013, which supported governmental research focused on the environmental behavior of non-conventional petroleum products, such as diluted bitumen.<sup>11</sup> Their findings, along with a study by the National Academy of Sciences, disproved the misconception that diluted bitumen rapidly sinks.<sup>2,11</sup> Rather, they showed that dilbit does not sink until a period of 21 days has passed. The main driving factor for the sinking of dilbit is interaction with fine sediments in the water column.<sup>11</sup>

Evaporation is an important weathering process affecting the bulk chemical composition of the oil in the initial hours or days following a spill. Compounds with boiling compounds below 270 °C, or that have vapor pressures greater than about 0.1 mm Hg (approximately up to n-tetradecane), tend to evaporate rapidly from the surface of spilled crude oil.<sup>12</sup> The extent to which evaporation will affect the composition of crude oil varies with the composition of the oil. For instance, a gasoline spill may evaporate completely within a few hours, while heavier crudes, which generally have already undergone extensive weathering, will experience minimal losses due to evaporation.<sup>9</sup> Physical weathering processes can also impact the rate of evaporation. For example, emulsification, the process in which small water droplets are incorporated into spilled oil (or vice versa), can substantially reduce the rate of evaporation of the more volatile compounds of oil.<sup>9</sup> In the case of dilbit, a heavy oil, emulsification will result in minimal losses due to evaporation.

Dissolution is a lesser factor than bulk composition changes of spilled oil compared to evaporation, due to the nonpolar nature of hydrocarbons. Studies have shown that evaporation dominates the losses of surface spills.<sup>13</sup> It has been estimated that dissolution will reduce the mass of crude oil by 1-3 wt%, while evaporation accounts for 10-50 wt%.<sup>14</sup>

In photochemical oxidation, the dominant chemical weathering process, UV rays can cleave some of the hydrocarbon bonds in oil or can create oxygen containing radical species in the air or water that can oxidize hydrocarbons. This processes most notably affects the PAHs, transforming them into more polar compounds with epoxide, carboxyl, and hydroxyl groups, which can lead to preferential dissolution into the water column.<sup>9</sup> The amount of photooxidation occurring is directly correlated with the intensity of incident UV Rays. Thus, most photooxidation occurs on the surface of oil slicks, and is highly dependent on the thickness of the slick, which is a function of the oil viscosity and how thinly it spreads on the surface of the water. Photochemical oxidation is also drastically reduced in dispersed oil

droplets deeper in the water column. There are also many different chemical pathways of PAH photochemical oxidation, resulting in a myriad of different products from one parent PAH (Figure 5).

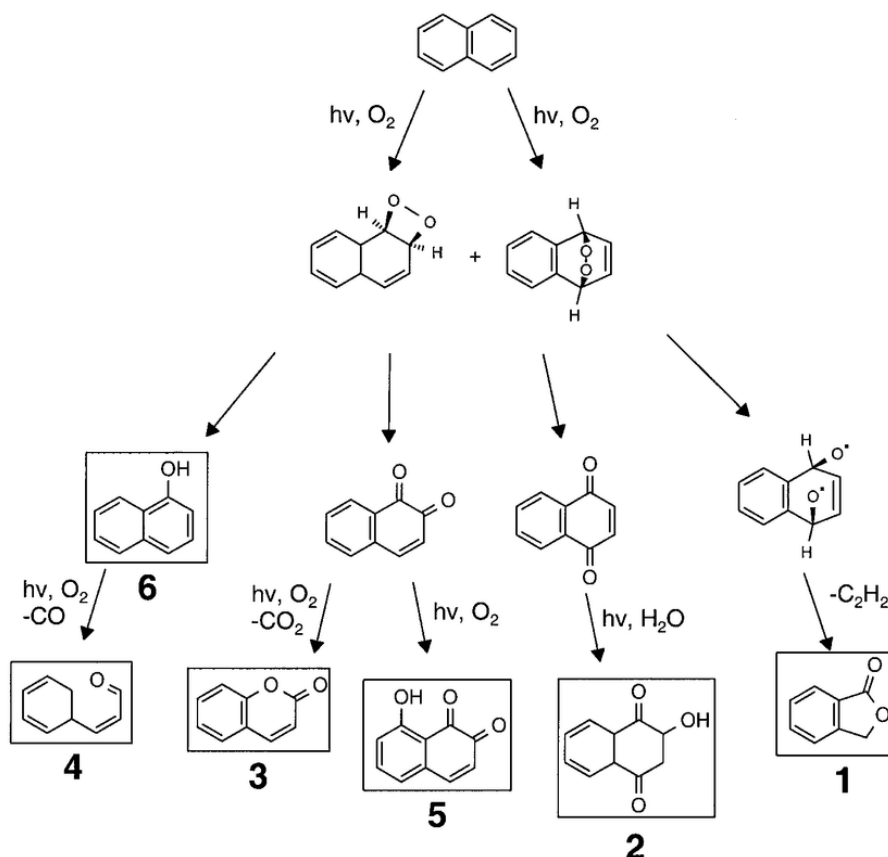


**Figure 5. Different chemical pathways for the photochemical oxidation of naphthalene<sup>15</sup>**

Since the first publication of microbial growth on petroleum<sup>16</sup>, the use of microorganisms to degrade petroleum has been a subject of extensive research. Following an oil spill, different hydrocarbon classes are degraded simultaneously, but at widely varying rates by indigenous microbiota.<sup>16</sup> Low molecular weight n-alkanes ranging from 10 to 22 carbons are biodegraded most rapidly, followed by saturated terpenoids and higher molecular weight n-alkanes, monoaromatics, PAHs, and finally, highly condensed cycloalkanes (hopane and sterane biomarker compounds), resins, and asphaltene.<sup>9</sup> In addition, parent PAHs are most rapidly biodegraded compared to their alkylated derivatives and sulfur heterocyclics such as dibenzothiophene.<sup>17</sup> The conditions of biodegradation are

highly variable, determined by ambient conditions such as the nature of the oil present, the temperature of the water, dissolved oxygen, the composition of the microbial community, and, of course, the composition of the crude oil.<sup>18</sup> Studies have suggested that heavy oils, which have likely biodegraded for millions of years in an oil reservoir, may be unaffected by microbial degradation.<sup>9</sup>

Hydrocarbons in their original state are not amenable to cellular metabolism. In order to transform the components of crude oil, hydrocarbons are activated through the addition of one or both atoms of diatomic oxygen by enzymes, respectively known as monooxygenases and dioxygenases. Once hydrocarbons are activated by these enzymes, they are generally directed into the lipid catabolic pathways of the cells<sup>9</sup>. Figure 6 below shows various molecules being activated by these enzymes. These enzymes transform hydrocarbons into numerous oxygenated products, including, but not limited to, alcohols, ketones, carboxylic acids, and epoxides.

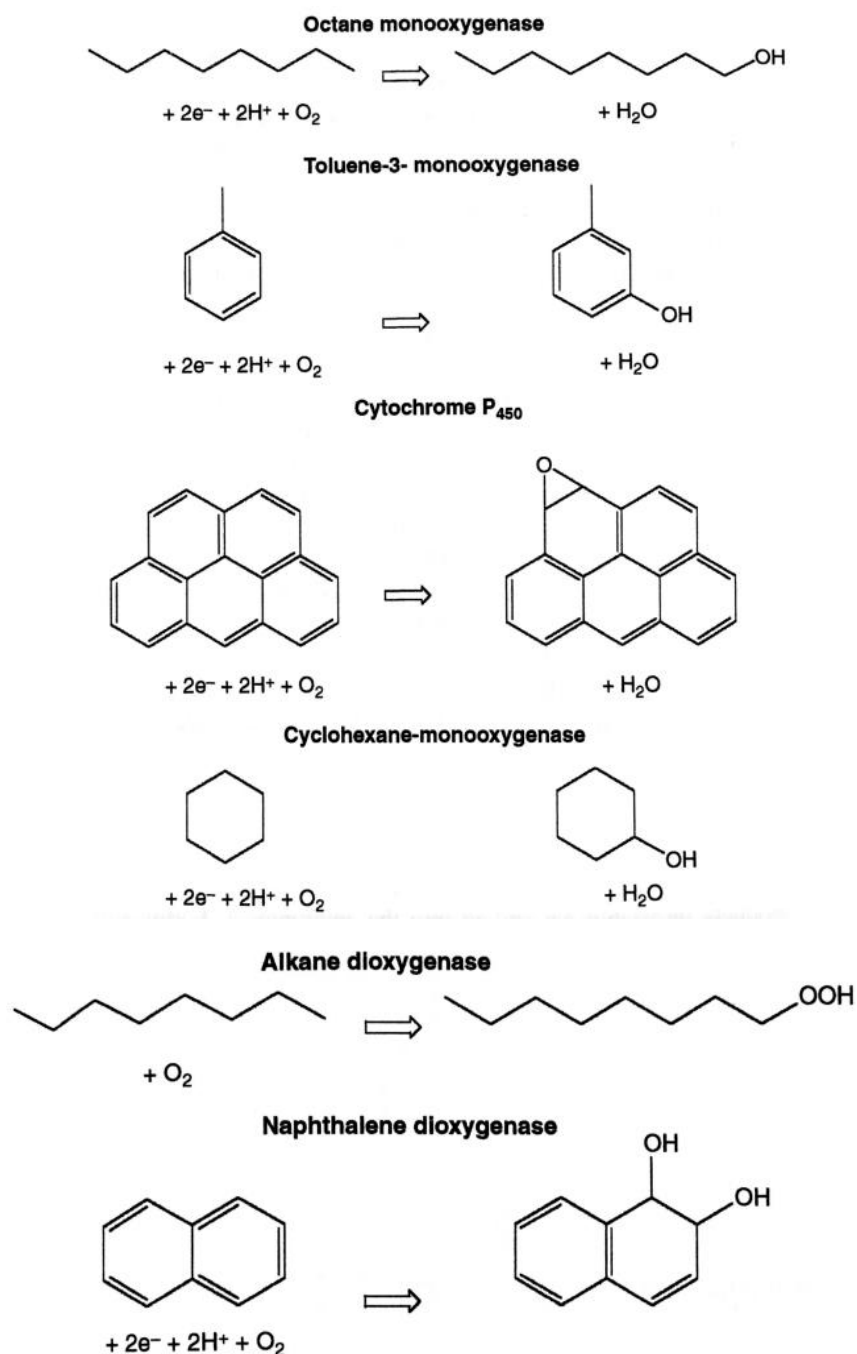


**Figure 6. Typical reactions catalyzed by hydrocarbon monooxygenases and dioxygenases (Stout, Wang, 2016)**

Although we'd like to study these enzymes in vitro separately, however they are very difficult to isolate from the microbial membranes, as many different oxygenase enzymes can be present in one cell. Many different factors control the extent and rate of oil biodegradation. For biodegradation to occur,

there must be terminal electron acceptors present, like molecular oxygen, nitrates, sulfates, ferric iron, or carbon dioxide.<sup>9</sup> Essential nutrients like nitrogen and phosphorus also must be available to encourage microbe growth. Bioremediation efforts often involve overcoming these nutrient limitations by addition of nitrates and phosphates.<sup>19</sup> Microbes cannot directly grow in petroleum; water must be present, although the amount can be exceedingly low.<sup>20</sup> The water must also be at the proper salinity and temperature to support microbial growth.

While other weathering processes like evaporation and photooxidation determine the short-term fate of spilled oil, microbial biodegradation is the ultimate long-term weathering process. Understanding biodegradation is critical to understanding the full environmental fate and impact of an oil spill and planning for effective responses. Many recent investigations into dilbit's spill behavior cite the need for more extensive research on the extent of its biodegradation.<sup>2,11</sup> Our research is aimed at closing this knowledge gap in order to fully understand the weathering of dilbit and the environmental conditions which may influence this process. Our goals of this work aim to develop a method to assess the short-term biodegradation of dilbit in the marine environment. The results of this work will enable future examination of the effect of temperature, salinity, nutrient availability, and microbial community, on the rate and efficacy of biodegradation and help inform the response to future spills.

### **3. Methods**

Previous experiments with lighter crude oils involved diluting the oil in a water-miscible solvent such as acetone and then adding this directly to the water samples. Attempts to do this with dilbit resulted in only a small fraction of the dilbit going in to solution. The solubility of dilbit with other solvents, including dichloromethane, 70:30 dichloromethane:methanol (v:v), and tetrahydrofuran was examined. The dilbit was soluble in these solvents, however, when the diluted oil solution was spiked into the seawater microcosms, the oil quickly partitioned to the glass surface above the water line, limiting its potential availability to microbes in the water.



To address this issue two microcosm set-ups were tested: a microcosm where the oil solution was spiked onto sand and then exposed to the water, and the creation of a water-accommodated-fraction (WAF) of oil. These separate experiments are described below.

### 3.1. Diluted bitumen samples

Two neat dilbit samples were obtained from Robyn Comny at the US EPA: an aliquot of the product spilled in the 2010 Kalamazoo River spill and an aliquot of dilbit from Cold Lake, a main source of oil sands in Alberta, Canada.

### 3.2. Sand Microcosm Experiment

The first experiment employed a microcosm method similar to one used by Sharma et al. (2016)<sup>21</sup>. A 230 mg/mL solution of the Kalamazoo Spill dilbit sample was prepared in pesticide-grade tetrahydrofuran. Approximately 28.75 mg of oil (125  $\mu$ L aliquots) were spiked directly on to approximately 5 g of sand in 60-mL vials, and filled with 40 mL of seawater, obtained from Charleston Harbor (Figure 7). All sand and glassware used was cleaned and sterilized by baking in a muffle furnace at 450 °C for 8 hours prior to use.

All water used in this experiment was used at room temperature. Three treatments of seawater microcosms were prepared. Autoclaved seawater was used as a negative control.

The remaining two seawater treatments were live seawater: native seawater, and seawater containing 2 mM ammonium chloride (CAS 12125-02-9) and 0.5 mM potassium phosphate (CAS 7778-53-2) nutrient spike. The results generated from these two live treatments will assess whether biodegradation is limited by Nitrogen or Phosphorus availability. Samples were capped with sterile cotton balls to prevent

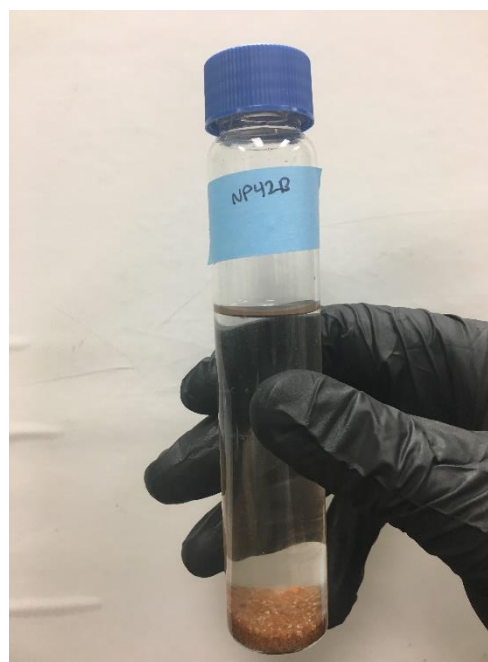


**Figure 7: Representative microcosm using sand method (nitrogen and phosphorus treatment, day 42, replicate B)**

contamination by particulates in the ambient air while allowing for oxygen exchange. Microcosms were placed in a vial rack and covered with foil to exclude any photooxidation that might occur, and were placed on a shake table to encourage the mixing of oil into the water (Figure 8). Samples were prepared in triplicate and extracted at day 0, 7, 14, and 21.

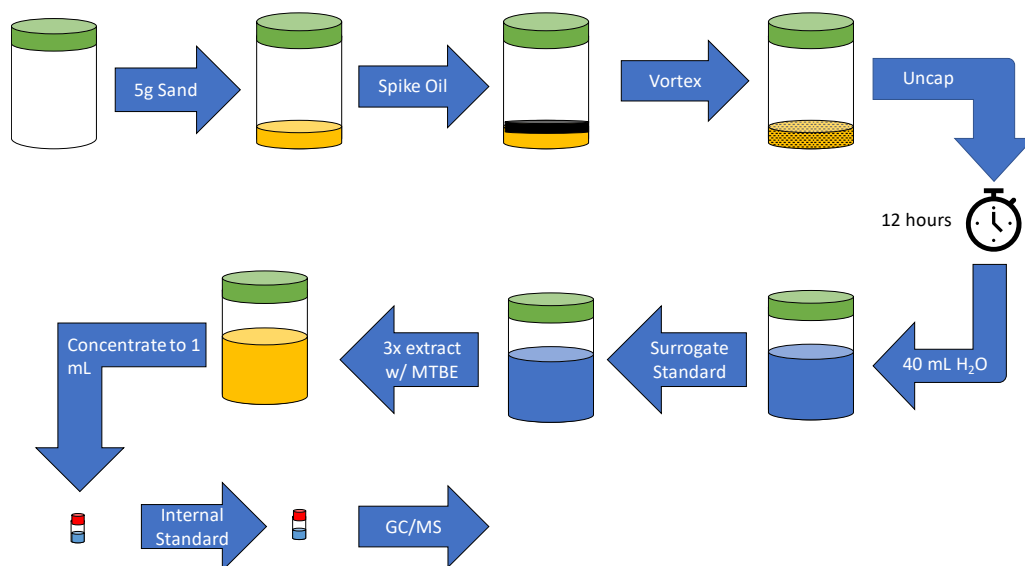


**Figure 8. Sand microcosm setup and extraction**

### 3.3. Water-Accommodated-Fraction Microcosm Setup

The second experiment employed another method to add a consistent amount of oil directly into the microcosm water by creating a water-accommodated fraction (WAF) of oil. This preparation method involves placing oil over a volume of seawater, followed by vigorous mixing and a settling period, resulting in a suspension of small oil droplets.<sup>22</sup> To prepare the WAF, 1 liter of Charleston Harbor seawater was passed through a GF/F glass fiber filter to prevent oil from adsorbing to any sediment. The water was then passed through a 0.2  $\mu\text{m}$  glass fiber filter to preclude any microbiological contamination. Approximately 10 g of Cold Lake dilbit were added to 700 mL of the filtered water in a separatory funnel and shaken vigorously for 1 minute, creating an emulsion (Figure 9). After two minutes of settling time, the WAF was added in 10 mL aliquots to each microcosm.

Two treatments of seawater were prepared for this setup: sterile seawater as a negative control and live. We initially planned to add a nutrient amendment to our live microcosms, however it was not added. Over the course of WAF addition, nine aliquots of the WAF were taken throughout the addition to the microcosms to monitor any possible decrease in the WAF concentration. Microcosms were covered in aluminum foil between extractions to minimize photooxidation. The microcosms were placed horizontally in the shake table to further improve mixing of the water at room-temperature. To prevent spilling, microcosms were tightly capped throughout the experiment (Figure 10). Microcosms were opened occasionally throughout the experiment to refresh the oxygen content.

Samples were prepared in triplicate and extracted at day 0, 7, 14, and 21. To monitor extraction efficiency, a surrogate standard stock containing 256  $\mu\text{g/g}$  deuterated heptadecane in dichloromethane. In each microcosm, 25  $\mu\text{L}$  of the surrogate standard solution was added prior to extraction, obtaining 50  $\mu\text{g/g}$  in the final extract. A stock solution containing 243  $\mu\text{g/g}$  of deuterated pentadecane in DCM was also prepared as an internal standard. Volumetric differences across samples were accounted for by adding 25  $\mu\text{L}$  of this solution to each concentrated extract, with a final concentration of 40  $\mu\text{g/g}$ .



**Figure 9. Preparation of the water-accommodated fraction**

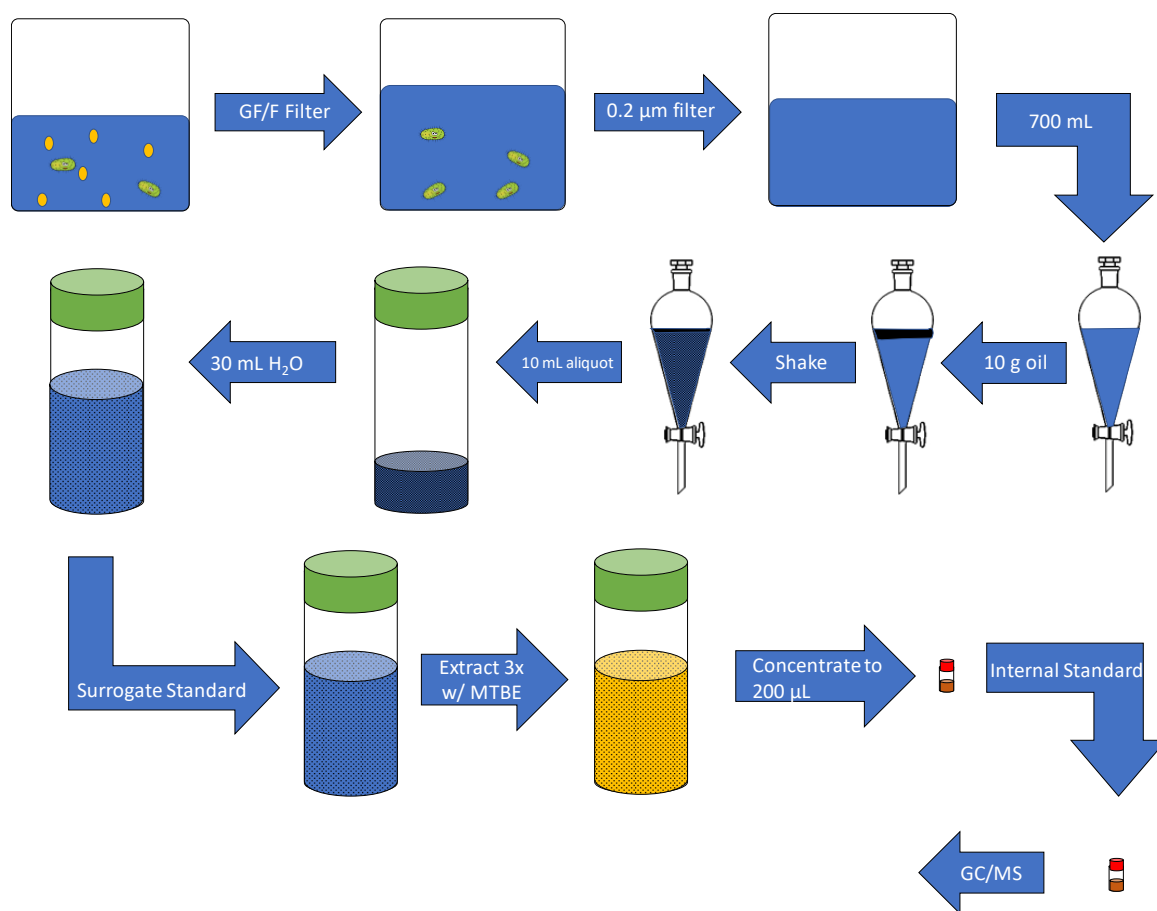


**Figure 10. WAF microcosm setup and extraction**

### 3.4. Microcosm Extraction

Samples were extracted with methyl tert-butyl ether (MTBE) at the aforementioned time points to monitor the effect of biodegradation throughout the course of the experiment. For each time point across treatments, microcosms were prepared in triplicate. Prior to extraction, samples were gravimetrically spiked with 5  $\mu\text{g}$  of deuterated heptadecane in 25  $\mu\text{L}$  as a surrogate standard. To extract the oil in each microcosm, 10 mL of MTBE was added to the microcosm vial and vortexed for 30 seconds. The organic layer was then pipetted through a glass wool filter to remove sediment. This was done three times for each microcosm, totaling 30 mL of MTBE per sample. The solvent extracts in the sand and WAF microcosms were concentrated to 1 mL and 200  $\mu\text{L}$ , respectively, using rotary

evaporation. The extraction methods are summarized in Figures 8 and 10 above for the sand microcosms and WAF microcosm respectively.

### 3.5. Standard Prep

To quantify the amount of oil within each microcosm, a set of calibration standards were made using a triacontane standard from sigma Aldrich.. Concentrations ranged from 0.076  $\mu\text{g/g}$  to 8.44  $\mu\text{g/g}$ . Table 1 below details the preparation of the calibration standards.

**Table 1. Calibration standard preparation**

Standard #	1	2	3	4	5
p triacontane stock, $\mu\text{g/g}$	1.390	1.390	1.390	1.390	1.390
mass stock added, g	0.014	0.027	0.064	0.129	0.200
mg triacontane added	0.019	0.038	0.090	0.179	0.278
mass solution, g	0.252	0.265	0.263	0.259	0.263
[triacontane], $\mu\text{g/g}$	0.076	0.142	0.341	0.690	1.056

### 3.6. GC-ToF-MS Analysis

Extracts were analyzed on an Agilent 7890 Series GC coupled to a LECO Pegasus time-of-flight mass spectrometer. Samples (2  $\mu\text{L}$ ) were injected in splitless mode and separated on a HP5-MS column (30 m length, 0.25 mm I.D, 0.25  $\mu\text{m}$  film thickness) with helium as a carrier gas at a constant flow of 1.10 mL/min. The temperature program of the oven started at 50  $^{\circ}\text{C}$  (10 min) and was then ramped from 50  $^{\circ}\text{C}$  to 170  $^{\circ}\text{C}$  at 5  $^{\circ}\text{C}/\text{min}$ , then held isothermally for 5 minutes. The oven was then ramped from 170  $^{\circ}\text{C}$  to 300  $^{\circ}\text{C}$  at 10  $^{\circ}\text{C}/\text{min}$ , then held isothermally for 10 minutes. The mass spectrometer used electron-impact ionization with an energy of -70 V, with an ion source temperature of 250  $^{\circ}\text{C}$ . A mass range of 50-600 m/z was analyzed at a frequency of 10 Hz at a detector voltage of 1500 V.

### 3.7. Data analysis

Table 2 below details a list of the analyzed compounds and their respective retention times and mass-to-charge ratios. They were identified by comparison to authentic n-alkane and PAH standards

purchased from Sigma Aldrich and established published peak orders. These compounds span a range of volatilities, solubilities and biodegradation potentials.

**Table 2. List of compounds in dilbit analyzed for both microcosm experiments with mass-to-charge ratios and retention times**

Analyte	m/z	Retention time, min.
Naphthalene	128	20.82
Deuterated pentadecane	66	29.34
pentadecane	57	32.27
Deuterated heptadecane	66	33.95
heptadecane	57	34.53
pristane	57	34.68
Dibenzothiophene	184	35.75
Phenanthrene	178	36.50
octadecane	57	37.32
phytane	57	37.62
Benz(a)anthracene	228	48.26
triacontane	57	51.52
Benzo(a)pyrene	252	51.98
Hopane	191	53.61

Several data-processing methods were employed to gauge biodegradation of the oil samples.

Compound-specific peaks were identified by analyzing the chromatogram at several different mass-to-charge ratios. Peak areas of specific compounds in each sample such as naphthalene, heptadecane, triacontane, and benz(a)pyrene were also normalized against the peak area of 17 $\alpha$ ,21 $\beta$ -hopane.

Hopanes are polycyclic saturated ring compounds found in every source of crude oil and are highly resistant to biodegradation (see figure 1) (Prentice Hall, 1993). Researchers often use hopane as a pseudo-internal standard, because it is shown to be the most recalcitrant biomarker compound in crude oil (Venosa, 1997). This allows researchers to account for differences in concentration of the oil extracts by using the ratio of hopane to other degradable peaks across an oil sample.<sup>3</sup> This ratio is used to generate compound-specific percent losses over time. The calculation for percent loss is shown below:

$$\% \text{ Loss} = \left( \frac{\text{Analyte Peak Area Day } n}{\text{Hopane Peak Area Day } n} \right) \times 100\% \quad (1)$$

The normalized hopane ratios for the live seawater treatments were compared to the negative control samples in order to correlate the percent loss of compounds across samples. If biodegradation is occurring, these hopane ratios should decrease over time.

Generally, complex branching hinders both the oxidation and lipid catabolism of hydrocarbons from occurring, due to steric hinderance with the enzymes.<sup>9</sup> Thus, branched alkanes are more resistant to biodegradation. By taking the ratios of specific alkanes and their branched (isoprenoid) equivalents over time, alkane biodegradation can easily be gauged. Two easily-identifiable sets of these are heptadecane (*n*-C<sub>17</sub>) to pristane, and octadecane (*n*-C<sub>18</sub>) to phytane. Biodegradation will decrease these ratios throughout the experiment, as the isoprenoids are more resistant to biodegradation.<sup>16,23</sup> Figure 11 depicts a chromatogram of a neat dilbit sample with these alkanes and isoprenoids identified.

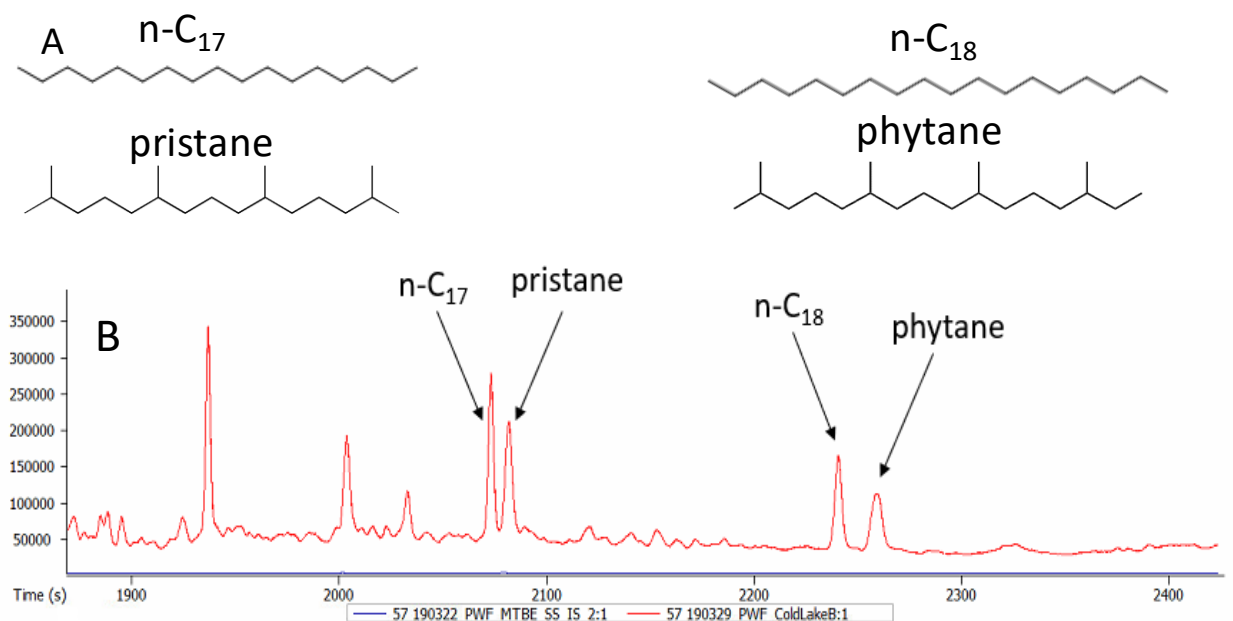


**Figure 11. (A) Chemical structure of *n*-C<sub>17</sub>, pristane, *n*-C<sub>18</sub>, and phytane. (B) Extracted ion chromatogram depicting *n*-C<sub>17</sub> and pristane, *n*-C<sub>18</sub> and phytane (*m/z* = 57)**

### 3.8. QA/QC

Throughout the GC-Tof-MS runs of each compound, several solvent blanks spiked with internal standard and surrogate standard were run as well.

To ensure that the WAF composition and concentration remained consistent over time, a Wilcoxon Rank Sum Test was performed on data obtained from the WAF replicates. A Wilcoxon Rank Sum Test is a useful tool for determining significant differences between small sample sizes. These tests compared the first and last 3 WAF replicates. WAF replicates were normalized to both hopane and the internal standard, to assess whether there was a statistically significant change in the oil composition concentration throughout the experiment, respectively. Using a type I error rate of  $\alpha = 0.05$ , there were no statistically significant differences in both the WAF composition and concentration throughout the addition.

Surrogate percent recoveries were calculated with the following equation:

$$\% \text{Rec} = \frac{\left( \frac{R_{SS}}{R_{IS}} \right)_{\text{sample}}}{\left[ \frac{\left( \frac{R_{SS}}{R_{IS}} \right)_{\text{std}}}{\left( \frac{\text{mass}_{IS}}{\text{mass}_{SS}} \right)_{\text{std}}} \right]} \times 100\% \quad (3)$$

Where  $R_{SS}$  is the area of the surrogate standard,  $R_{IS}$  is the area of the internal standard,  $\text{mass}_{IS}$  is the average amount of internal standard added to the calibration standards, and  $\text{mass}_{SS}$  is the average amount of surrogate standard added to the calibration standards.  $\left( \frac{R_{SS}}{R_{IS}} \right)_{\text{sample}}$  was calculated for each

sample, while  $\frac{\left( \frac{R_{SS}}{R_{IS}} \right)_{\text{std}}}{\left( \frac{\text{mass}_{SS}}{\text{mass}_{IS}} \right)_{\text{std}}}$  was calculated for each calibration standard then averaged for use in the

equation. Gravimetric addition data was not obtained for the sand microcosm method, thus the surrogate percent recoveries were calculated based on response factors alone. In the sand microcosm



experiment, percent recoveries ranged from 9% to 113%, with an average recovery of 87.8%. The percent recoveries for each microcosm can be seen in table 3 below. Samples with percent recovery below 60% were excluded from analysis.

**Table 3. Surrogate recoveries for all extracted sand microcosms (Nomenclature: d=Dead, L=live, NP = nitrogen and phosphorus, number = day extracted A-C = replicate microcosms)**

Sample ID	% Recovery	Sample ID	% Recovery	Sample ID	% Recovery
D0A	97	L0B	73	NP0A	105
D0B	100	L0C	84	NP0B	102
D0C	96	L3B	94	NP0C	97
D3A	114	L3C	87	NP3A	61
D3B	103	L7A	47	NP3B	103
D3C	98	L7C	86	NP3C	97
D7A	95	L14A	80	NP14A	87
D7B	93	L14B	71	NP14B	9
D14A	54	L14C	113	NP14C	43
D14B	72	L21A	94	NP21A	79
D21A	101	L21B	88	NP21B	98
D21B	93	L21C	99	NP21C	109
D21C	99				

\*Some values missing due to spills or rotary evaporation to dryness

In the WAF experiment, surrogate recoveries ranged from 69% to 126%, with an average recovery of 93.3%. A summary of the surrogate recoveries can be found in table 4 below.

**Table 4. Surrogate recoveries for all extracted microcosms (WAF)**

Sample ID	% Recovery	Sample ID	% Recovery
DOA	125.99	LOA	82.65
DOC	96.28	LOB	82.31
D3A	93.45	L3A	90.56
D7A	90.75	L7A	94.74
D7B	97.03	L14A	105.91
D7C	102.67	L14B	104.52
D14A	N/A*	L14C	92.82
D14B	94.92	L21A	84.98
D14C	65.29	L21B	89.68
D21A	91.74	L21C	93.92
D21B	94.16		

\*D14A did not have surrogate standard added to it

\*Some samples missing due to no oil addition, evaporation to dryness, or spills.

### 3.9. Microbial Analysis

To confirm the presence of alkane-degrading bacteria, 2 L of seawater were passed through a 0.2 µm glass-fiber filter. The filter was grinded in DNA buffer, and bacterial genomic DNA was extracted using a Qiagen DNA Minikit according to the manufacturer's instructions. DNA purity and yield were quantified using a NanoDrop spectrophotometer (Thermo). However, no DNA was obtained from these filters.

If DNA is successfully obtained in future experiments, a polymerized chain reaction (PCR) can be performed using a method described in Wang 2010 to detect the *alkB* gene.<sup>24</sup> This PCR can be performed using two sets of primers. The first pair of primers consists of *alkBwf* (5'-AAYACNGCNCAYGARCTNGGVCAYAA-3'), and *alkBwr* (5'-GCR TGRTGRTCHGARTGNCGYTG-3'). The second primer pair consists of *monf* (5'-TCAAYACMGSNCAYGARCT-3') and *monr* (5'-CCGTARTGYTCNAYRTARTT-3'). These two sets of degenerate primers were designed based on the N-

and C-terminal domains of the bacterial genome.<sup>24</sup> Expected products at 550 and 420 bp would be generated from these primers. A PCR mastermix containing 0.05 U/ $\mu$ L Taq DNA polymerase, reaction buffer, 4mM of  $MgCl_2$ , and 0.4 mM of each dNTP (dATP, dCTP, dGTP, and dTTP), can be used to perform the PCR. Cycling would be performed with an initial denaturation for 5 min at 94°C followed by 32 cycles of 30 s at 94°C, 30 s at 50–55°C, and 45 s at 72°C and a final elongation step for 5 min at 72°C. Finally, the PCR products can be separated in a 1.0% agarose gel.

## 4. Results

### 4.1. Sand Microcosm Experiment

#### 4.1.1. GC-ToF-MS Chromatogram Time Series

The neat oil and a day 0 sample from the sand microcosm experiment were examined to detect any differences in oil composition once added to the microcosms (Figure 12). One of the notable differences is the presence of peaks at 1170s and 2860s in the day 0 sample. The ChromaTOF software has a feature where unknown peaks can be referenced through a library of known compounds. These peaks correspond with alkyl alcohols, like octanol and nonanol. We are not sure why these are present. There may have been a rapid oxidation of these alkanes, or rather the presence of dead cellular material in the seawater. To test this hypothesis, we recommend extracting an oil sample in water that has been precluded of bacteria.

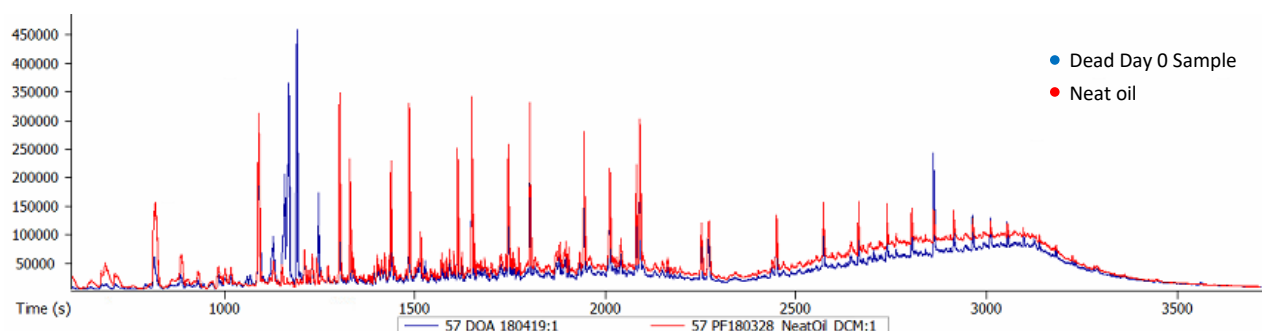


**Figure 12. Chromatogram overlay of neat oil and dead day 0 sample**

Data were collected for 21 days of the experiment. Chromatograms of the day 21 samples were normalized using the internal standard, and the overall shape of the chromatograms were analyzed to view the overall change in the composition over time (Figure 10). In both the alkane (Figure 13A, m/z 57) and PAH (Figure 13B, m/z 128, 152, 153, 166, 184, 178, 202, 228, 252, 276) extracted ion chromatograms, it is difficult to ascertain whether biodegradation occurred in the microcosms. The alkane and PAH chromatograms are composed of numerous, low-concentration coeluting compounds with similar mass spectra.

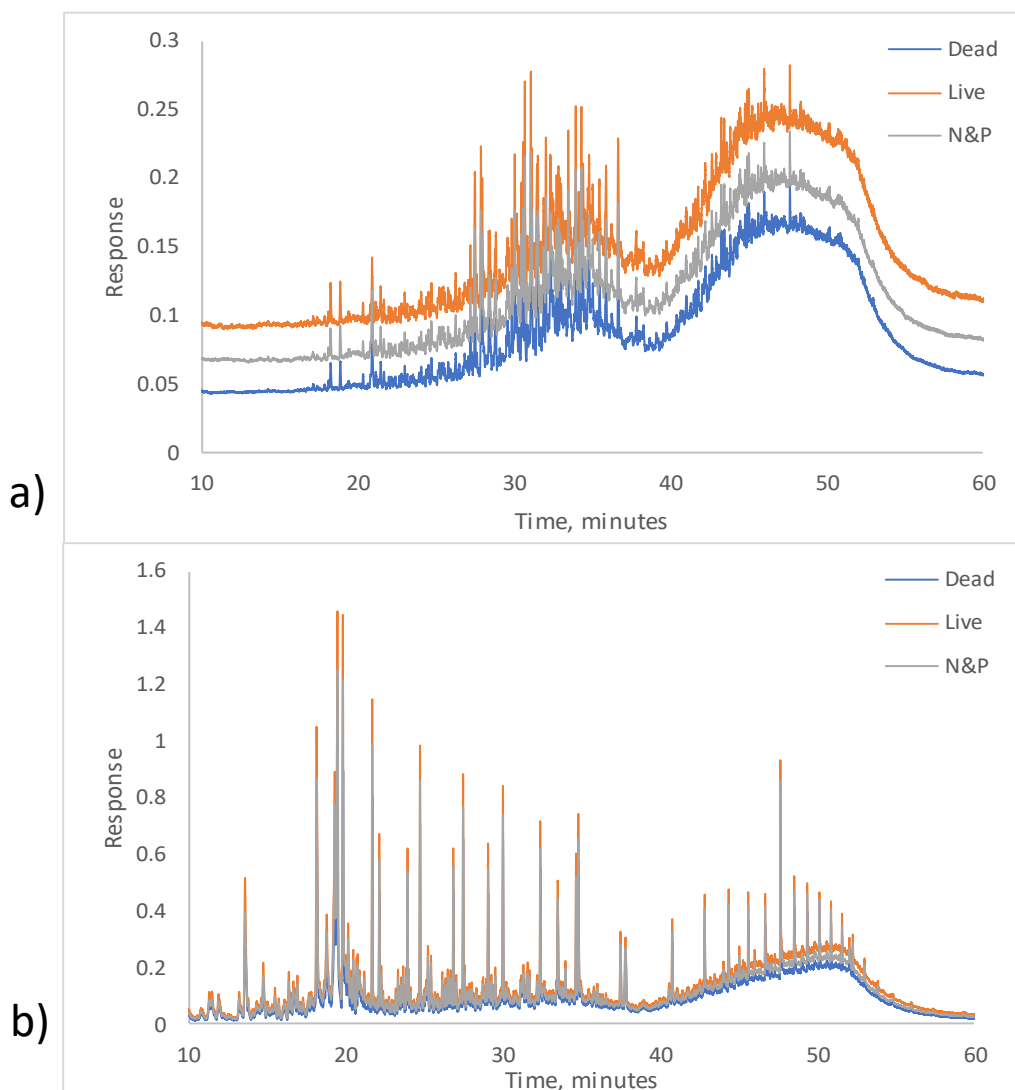


**Figure 13. Sand microcosm experiment chromatograms comparing day 21 samples for (a) the total PAH signature (m/z = 128, 152, 153, 166, 184, 178, 202, 228, 252, 276), and (b) the alkane signature (m/z 57)**

#### 4.1.2. Biodegradation Indicators

Due to the recalcitrance of the isoprenoids relative to their alkane counterparts, a ratio can be taken between the two to gauge alkane biodegradation. The  $n\text{-C}_{17}$ /Pristane and  $n\text{-C}_{18}$ /Phytane ratios for each treatment remained constant throughout the course of 21 days, suggesting that negligible amounts of alkanes were degraded (Figure 14)

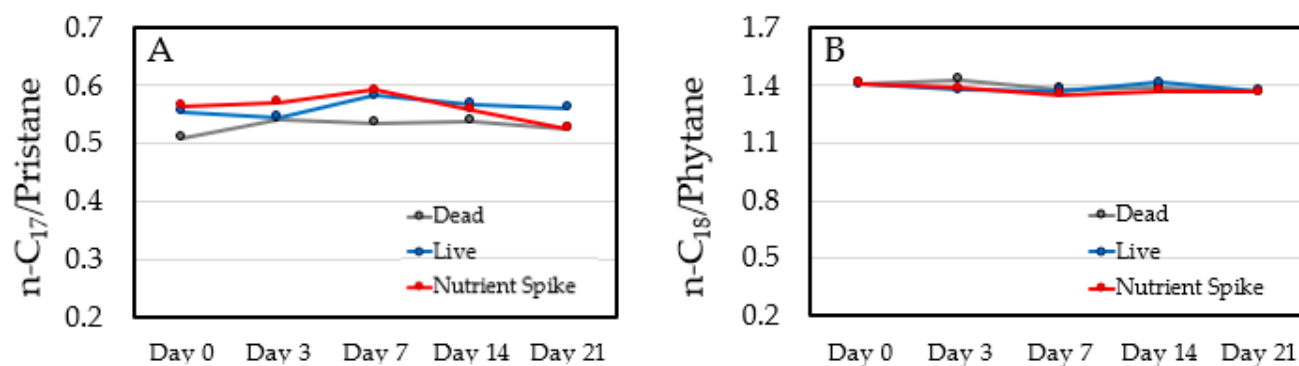


**Figure 14. Traditional indicators of alkane biodegradation for (A)  $n\text{-C}_{17}$ /pristane and (B)  $n\text{-C}_{18}$ /phytane ratios for dilbit samples over the course of 21 days.**

After normalizing the data to each sample's respective hopane peak area, the percent losses of the live treatments were compared to the negative control using a ratio of their compound's peak responses to compare compound-specific losses between the two live treatments (Figure 15). Across the live treatments there was little evidence of compound-specific biodegradation by day 21, except for naphthalene, with 50 % remaining. This was likely due to how the oil was added to the sand. Previous attempts at conducting this experiment involved adding the oil to the surface of the water, but the dilbit quickly adsorbed to the sides of the 60-mL vials, above the water mark. In this experiment the oil was added directly to the sand, adsorbing to it rather than dispersing into the water column. Naphthalene, which has a lower adsorption equilibrium constant, was able to partially disperse into the water column, and may have been degraded, or simply evaporated. As there was a lack of biological studies performed during this experiment, it's difficult to ascertain whether microbes were present at all. If there were, the

other components of the oil were likely strongly adsorbed to the sand in the microcosm, thus inaccessible by the microbes present in the water. If these compounds were degraded in the water column, the extraction process recovered most of the untouched oil from the sand. This likely masked any noticeable biodegradation of these compounds.

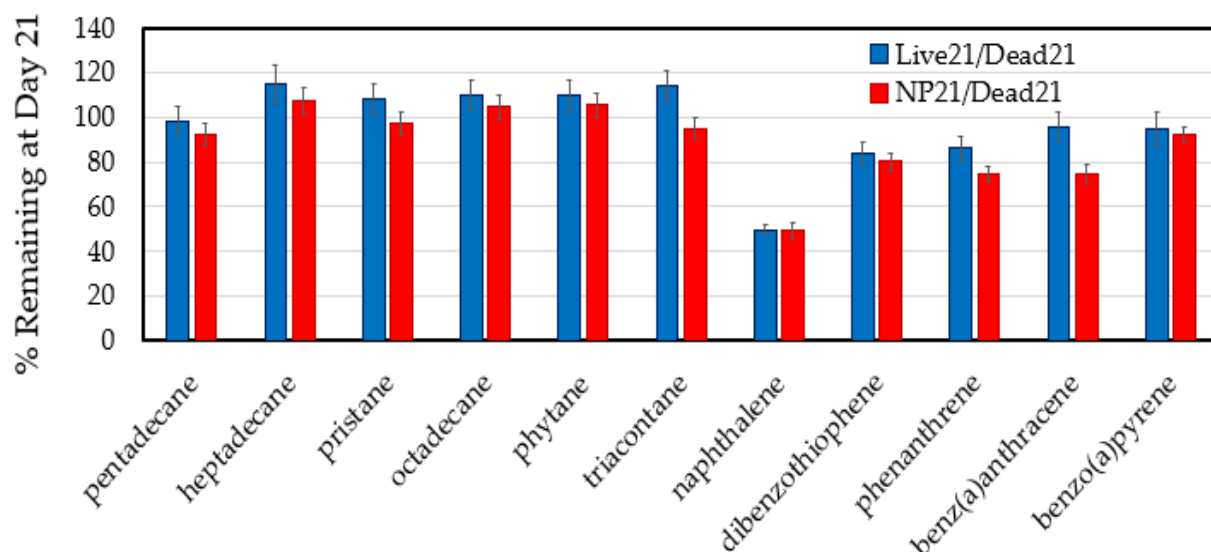


**Figure 15. Hopane-normalized concentrations of alkanes and PAHs in live and nutrient spiked (NP) treatments at day 21 compared to the negative control (Dead).**

## 4.2. WAF Microcosm Results

### 4.2.1. Oil Quantification

Attempts at recovering the bulk oil that was not accommodated by the WAF were unsuccessful, as there was residual water present in the oil that could not be removed by rotary evaporation. Instead, the alkane standard calibration curve was used. Because hopane is a 30-carbon molecule, we used a calibration curve for triacontane (Figure 16) and related that to the hopane concentration in the neat oil, as well as the WAF samples.

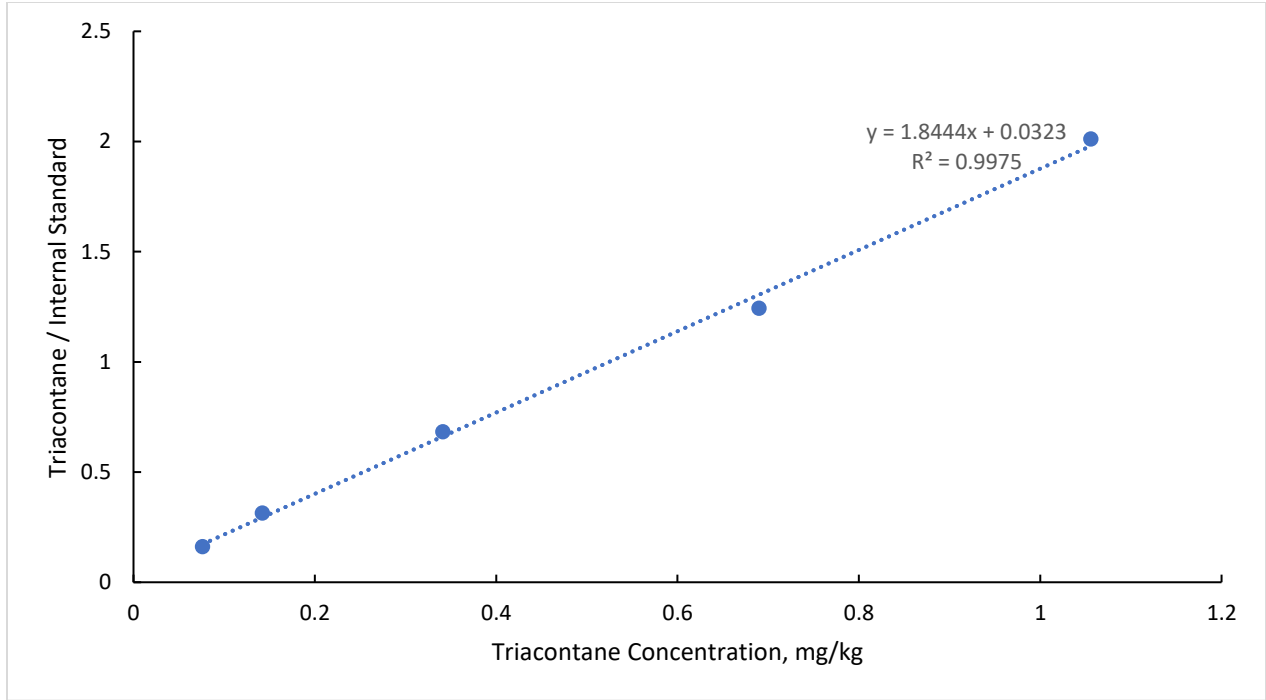


**Figure 16. Internal standard normalized calibration curve for triacontane**

The ratio of the total mass of hopane in the WAF and the total mass of hopane in the crude oil was taken to determine what fraction of the oil made it into solution. The calculation is as follows:

$$mH_{\text{totalcrude}} = \frac{mH}{m\text{Soln}} \times \frac{m\text{Soln}}{m\text{Oil}} \times m\text{Oil}_{\text{added}} \quad (4)$$

Where  $mH_{\text{totalcrude}}$  is the total mass of hopane in the oil added,  $\frac{mH}{m\text{Soln}}$  is the calibration curve-derived concentration of hopane in the neat oil sample,  $\frac{m\text{Soln}}{m\text{Oil}}$  is a fraction of the mass of the total neat oil solution in mg divided by the mass of oil added to the neat solution in mg, and  $m\text{Oil}_{\text{added}}$  is the total mass of oil added in the WAF creation in mg.

The calculation for total hopane mass in the WAF samples is as follows:

$$mH_{\text{WAF}} = \left( \frac{mH}{m\text{Soln}} \right)_{\text{WAF}} \times m\text{Soln} \times \frac{700 \text{ mL}}{10 \text{ mL}} \quad (5)$$

Where  $mH_{WAF}$  is the total mass of hopane in the WAF,  $\left(\frac{mH}{mSoln}\right)_{WAF}$  is the average calibration curve-derived concentration of hopane in the WAF samples,  $mSoln$  is the total mass of the WAF solution in kg, 700 mL corresponds to the total volume of the WAF, and 10 mL corresponds to the volume of the aliquots in each microcosm. For the WAF experiment, the ratio of  $mH_{WAF}$  to  $mH_{totalcrude}$  was 0.024, or 2.4 percent. For 9.8668 grams of oil added to the WAF, only 0.243 grams made it into solution.

#### 4.2.2. GC-ToF-MS Chromatogram Time Series

Similar to the sand microcosm, there was a distinct difference between the neat crude oil (Cold Lake) and the WAF samples, most notably seen by peaks at 1200 and 2750 s in the corresponding total ion chromatograms (Figure 17). We believe this could be due to preferential dissolution of dilbit in the seawater, or residual microbial cells present in the seawater that was extracted. More work is needed to discern this.

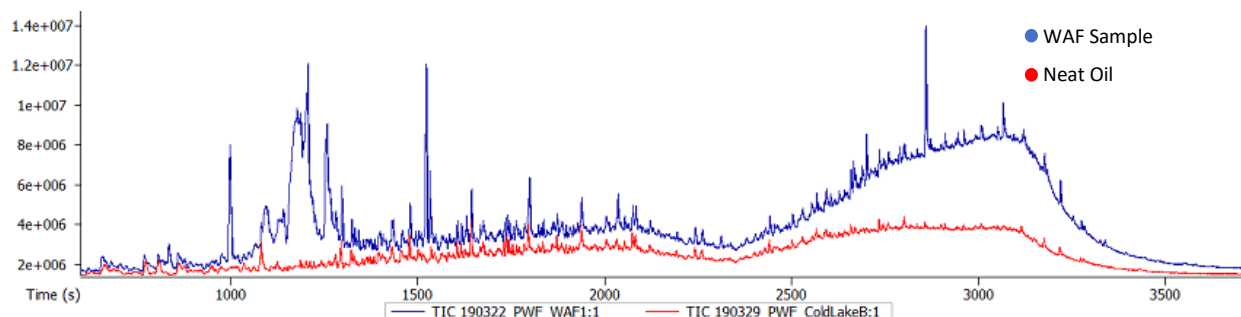


**Figure 17. Neat Cold Lake dilbit sample (blue trace) and WAF sample (red trace) GC-ToF-MS total ion chromatogram.**

Chromatograms for the WAF experiment were background-subtracted using the solvent blank, ensuring that they start at the same response. Chromatograms were also normalized to hopane. The TIC chromatograms for the dead microcosms can be seen in figure 18 below. There is a noticeable decrease of the unresolved complex mixture (UCM), the large unresolved region of co-eluting compounds between 40 to 60 minutes, over the course of 21 days.



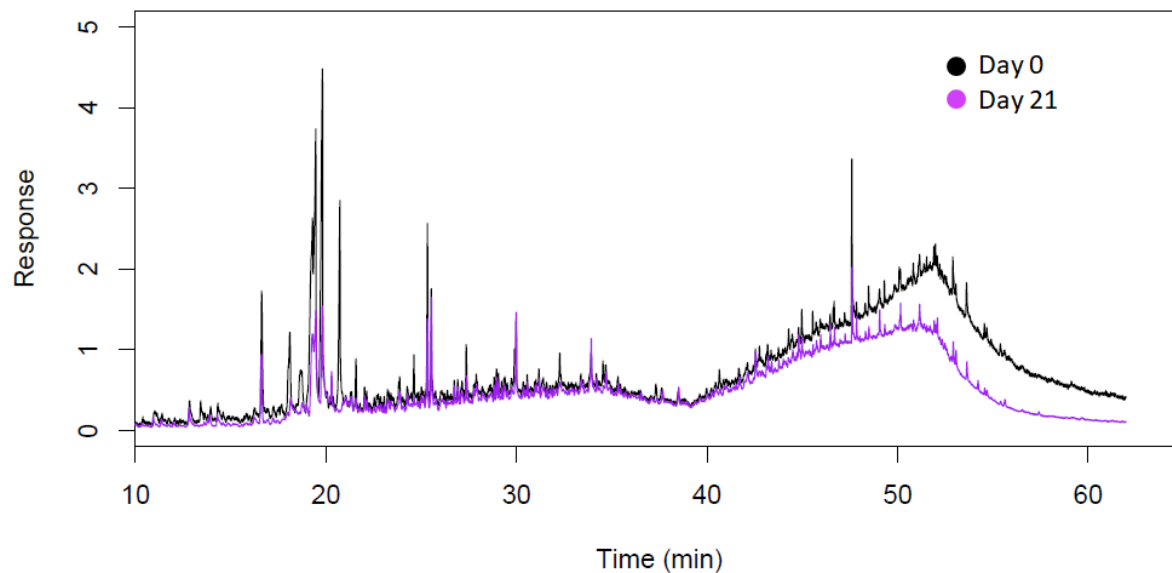


**Figure 18. Dead sample chromatograms at Day 0 (Black) and Day 21 (Purple) normalized to hopane**

Figure 19 below shows the EIC of alkane region ( $m/z = 57$ ) of the normalized dead samples.

There appears to be a decrease of resolved peak area over time.

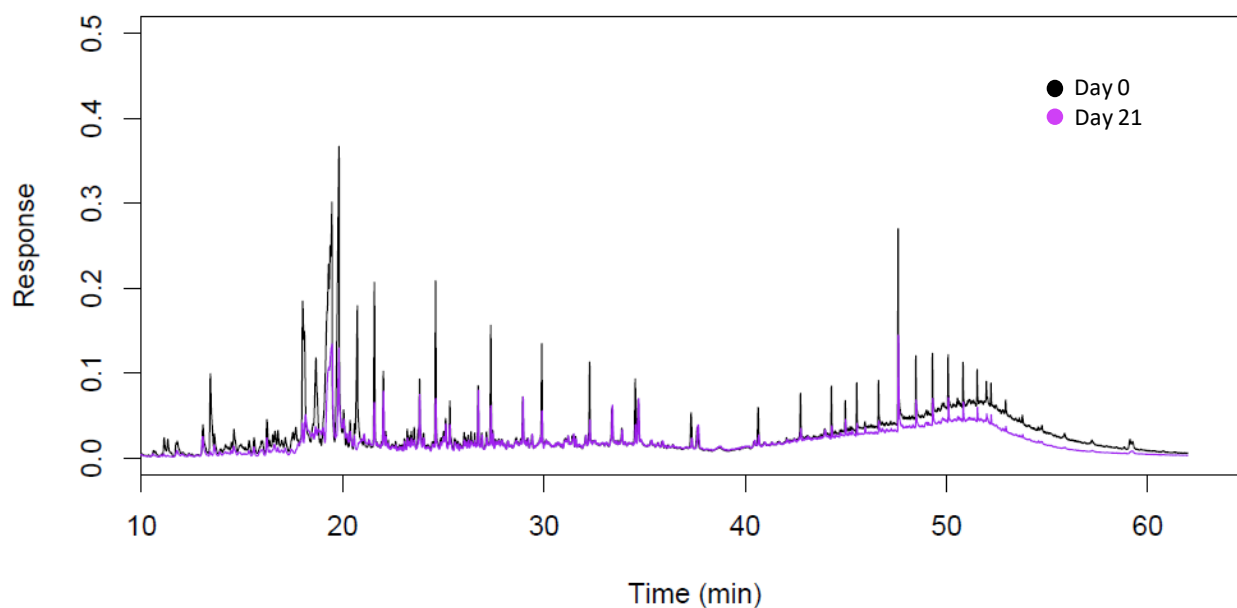


**Figure 19. Extracted ion chromatograms depicting the alkane region ( $m/z=57$ ) of dead microcosms at day 0 (black) and day 21 (purple) normalized to hopane**

The PAH chromatograms ( $m/z = 128+152+153+166+184+178+202+228+252+276$ ) for the dead samples can be found in Figure 20 below. Based on the chromatograms alone, there is little evidence of biodegradation occurring.

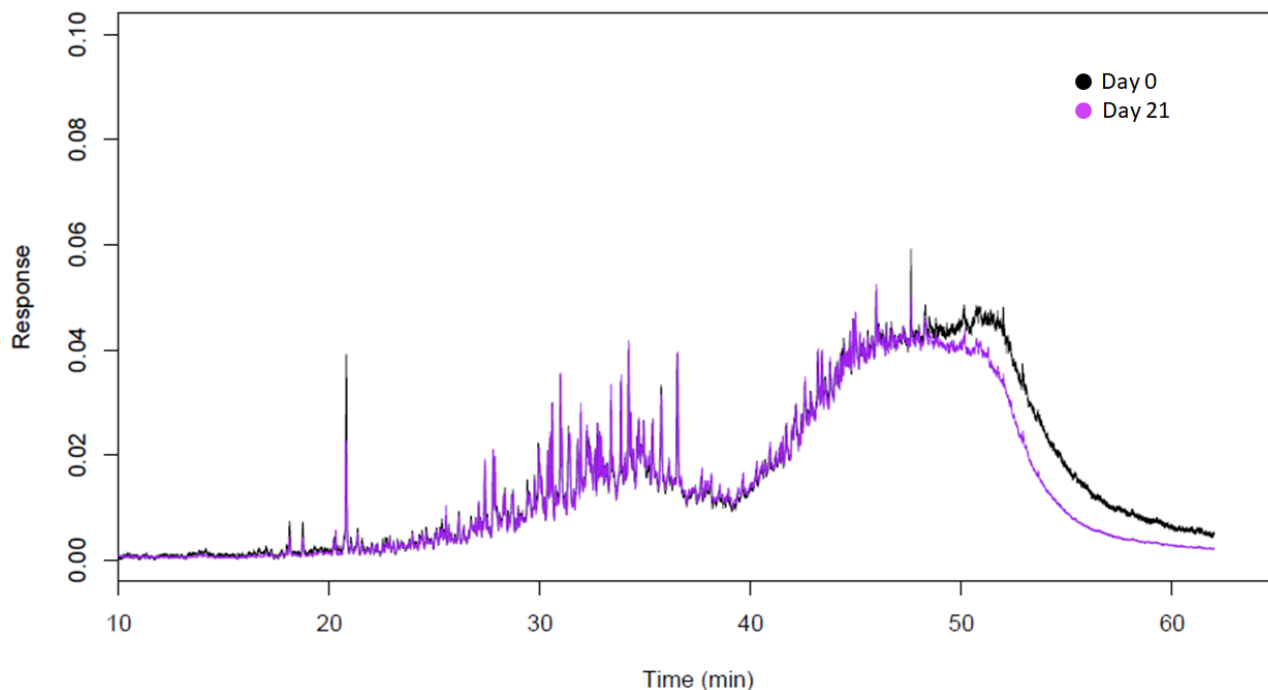


**Figure 20. Extracted ion chromatograms of the PAH region ( $m/z = 128 + 152 + 153 + 166 + 184 + 178 + 202 + 228 + 252 + 276$ ) of dead microcosms at day 0 (black) and day 21 (purple) normalized to hopane**

The total area of the background-subtracted, hopane-normalized chromatograms for the entire time series was calculated (Table 5). These values suggest that biodegradation occurred in the alkane region, but not the PAH region. We believe that there was a contamination in the water accommodated fraction that caused early biodegradation of the dead samples, but not PAH, as this region takes over 14 days to degrade.<sup>9</sup>

**Table 5. Total peak areas for TIC, alkanes, and PAH region of dead microcosms**

Region	D0 TIC	D7 TIC	D14 TIC	D21 TIC
TIC	36.27555	37.67973	39.46541	24.68199
Alkanes	1.433864	1.489514	1.588426	1.006592
PAH	0.797226	1.035829	0.332948	0.713941

The TIC of the live microcosms is shown in figure 21 below. Similar to the dead microcosms, there is a noticeable decrease in the UCM over the course of 21 days.

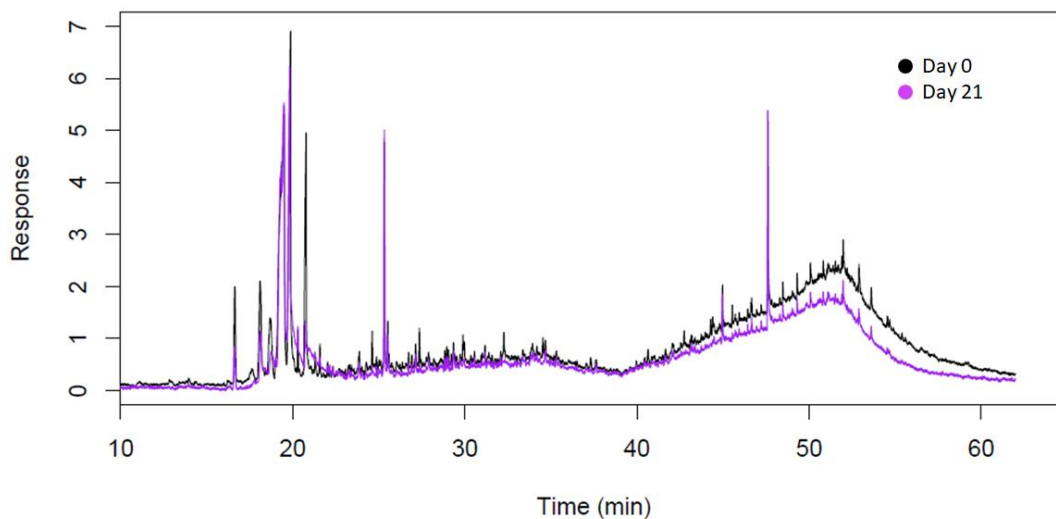


**Figure 21. Live sample TIC chromatograms at day 0 (black) and day 21 (purple) normalized to hopane**

The alkane region of the live microcosms show distinct losses in the resolved peak areas (Figure 22). This strongly suggests that biodegradation occurred over the course of 21 days.

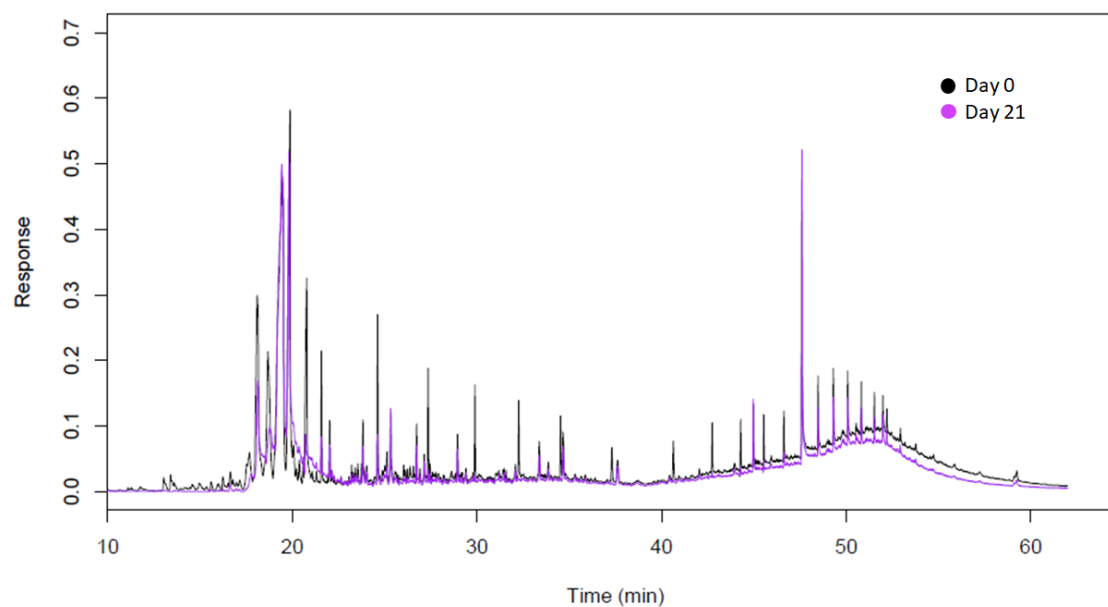


**Figure 22. Extracted ion chromatogram of the alkane region ( $m/z = 57$ ) of live microcosms at day 0 (black) and day 21 (purple) normalized to hopane**

The PAH chromatograms of the live chromatograms (Figure 23) show a major loss in both resolved peaks and the UCM. At a glance, this strongly suggests biodegradation occurring.

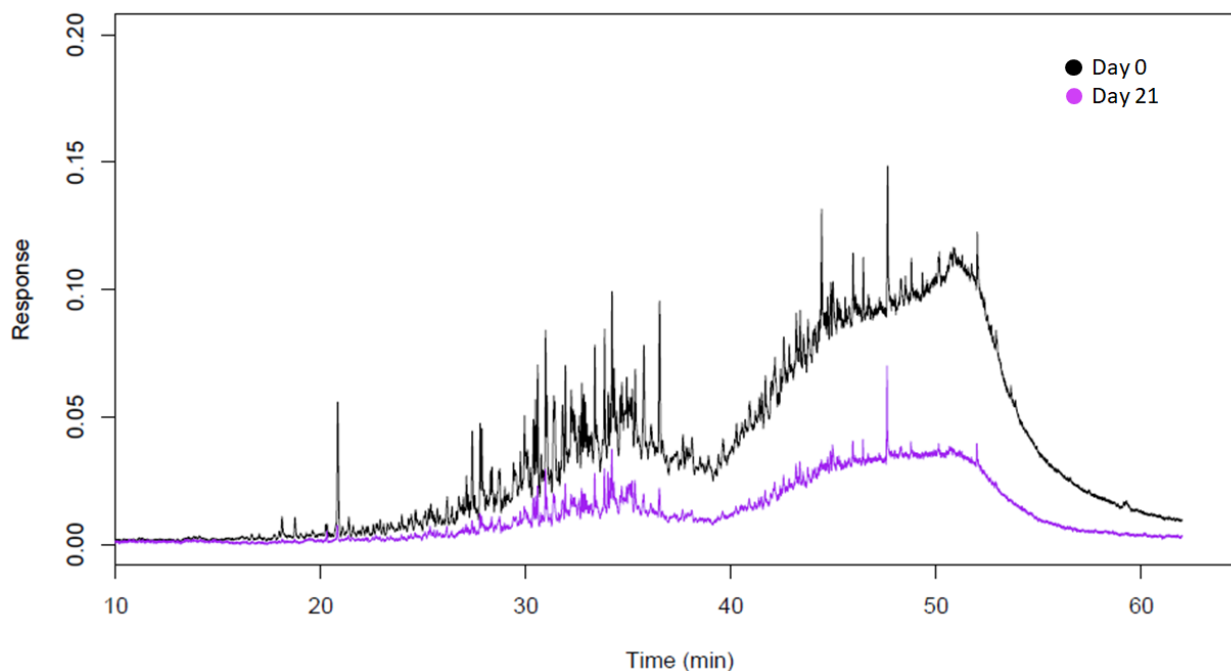


**Figure 23. Extracted ion chromatogram of the PAH region ( $m/z = m/z = 128 + 152 + 153 + 166 + 184 + 178 + 202 + 228 + 252 + 276$ ) of live microcosms at day 0 (black) and day 21 (purple) normalized to hopane.**

The total peak area of the live microcosms (Table 6) correlates well with the chromatogram time series, showing significant losses of each region analyzed.

**Table 6. Total peak areas for TIC, alkanes, and PAH region of dead microcosms**

Region	Day 0	Day 7	Day 14	Day 21
TIC	41.22788	47.52068	43.77912	31.42925
Alkanes	1.947751	1.810206	1.664948	1.506518
PAH	1.863498	1.162421	1.157035	0.624982

#### 4.2.3. Biodegradation Indicators

The  $n\text{-C}_{17}$ /pristane ratios for the WAF microcosms can be seen in figure 24 below. Over the course of 21 days, this ratio decreased in the live and dead treatments from 1.06 ( $\pm 0.02$ ) to 0.055 ( $\pm 0.004$ ) and 1.11 ( $\pm 0.03$ ) to 0.3 ( $\pm 0.14$ ), respectively.

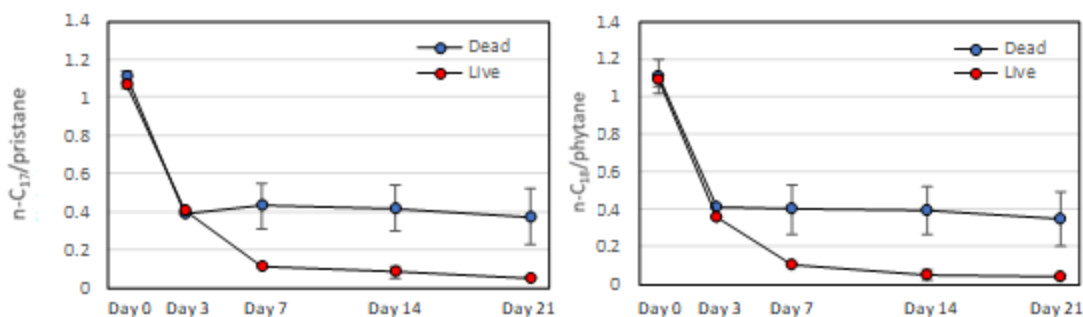


**Figure 24. Traditional indicators of alkane biodegradation for (A) n-C<sub>17</sub>/pristane and (B) n-C<sub>18</sub>/phytane ratios for dilbit samples over the course of 21 days.**

These alkane:isoprenoid ratios are indicative of biodegradation having occurred (Venosa, 1997) in the live sample. Unfortunately, the same trend can be seen in the dead samples however to a lesser extent. Because the dead seawater was autoclaved prior to addition to the microcosms, there was likely a contamination in the WAF itself. The seawater for the WAF was successively filtered through the GF/F and 0.2  $\mu\text{m}$  filters without rinsing the vacuum filtration apparatus between. It is likely that some of the microbiota passed through the first filter and contaminated the glass frit on the filter apparatus and therefore contaminated the WAF when it was passed through the 0.2  $\mu\text{m}$  filter. This error is a simple fix for future experiments. The alkane:isoprenoid ratios in the dead microcosms seem to level off after three days, suggesting biodegradation may have stopped shortly after addition of the WAF to the sterilized microcosms. This may explain why there was no noticeable loss in the PAH region of the dead microcosms, as PAH are more slowly degraded after a period of 14 days.<sup>9</sup>

Percent loss was calculated by dividing the average normalized live signal at day 21 by the average normalized dead signal at day 21 (Figure 25). This method of calculating percent loss, compared to dividing by the day 0 sample, accounts for potential losses not associated with

biodegradation. The alkanes showed considerable losses, except for triacontane, with 10 ( $\pm 10$ ), 20( $\pm 30$ ), and 10 ( $\pm 30$ ) percent remaining for pentadecane, heptadecane, and octadecane, respectively. We are unsure why triacontane has such a high value. The PAH region, although more variable, show 40 ( $\pm 60$ ), 50 ( $\pm 40$ ), 50 ( $\pm 50$ ), and 64 ( $\pm 1$ ) percent remaining by day 21 for naphthalene, dibenzothiophene, phenanthrene, and benz(a)anthracene, respectively. To reduce the variability in these values, we recommend using a greater number of replicate microcosms in the experiment.

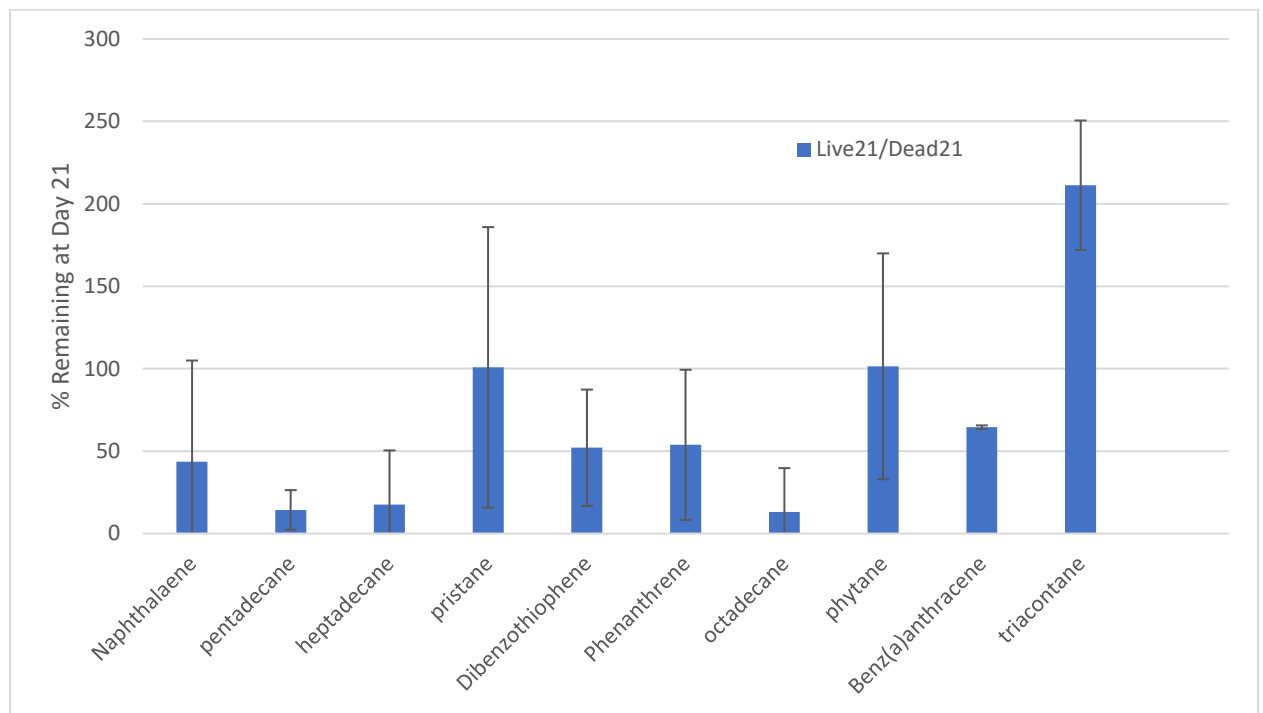


**Figure 25. Hopane-normalized losses for the WAF microcosms.**

#### 4. Implications and Future work

Results from the sand and WAF microcosm experiments have several implications when considering the design for future experiments. The lack of biodegradation seen in the sand microcosms suggests that adsorption to sediment vastly reduces the bioavailability of spilled oil. By sterilizing the sand used in this experiment, any bacteria that may have been available to facilitate biodegradation

were killed off, as well. To successfully incorporate sediment into future biodegradation studies, it is recommended that sediment native to the seawater sampling site be collected as well.

Despite a contaminated dead seawater treatment, the use of a WAF to distribute oil into each microcosm was a success. This contamination can easily be avoided in future experiments by washing out the filter apparatus prior to passing the seawater through the 0.2  $\mu\text{m}$  filter or using a separate sterile vacuum filtration apparatus. Results from the Wilcoxon Rank Sum test showed that there were no statistically significant differences in the oil concentration between WAF replicate samples. Thus, it is recommended that this method be used in future experiments examining biodegradation in the water column.

There were two assumptions made about the WAF microcosms during the experiment: that they were not nutrient limited, and that the occasional burping of the microcosms allowed sufficient amounts of oxygen to be replenished. In order to isolate these variables, future experiments should include more treatments, like the addition of a nitrogen and phosphorus amendment to the seawater. While the nutrient amendment did not show increased biodegradation in the sand microcosms, there is significant literature documenting the importance of these nutrients.<sup>8</sup> Dissolved oxygen levels can be monitored using an oxygen meter as described in Shrestha et al. (2019) to ensure that conditions are appropriate for aerobic biodegradation.<sup>25</sup>

The uptake of PAH by microbes may be facilitated by photooxidation, as oxidized molecules are more accessible to lipid catabolism.<sup>8</sup> To test this hypothesis, the WAF experiment should be repeated with the addition of a set of samples exposed to UV light. Performing a phospholipid fatty acid (PLFA) extraction of the microcosms as described in Bostic et. al (2018) will give a snapshot of the viable microbial community as well as the type of oil compounds are incorporated into their lipid

membranes.<sup>14</sup> Appropriate mass-to-charge ratios can be monitored for these oxidized PAHs to calculate what extent PAHs are biodegraded under these conditions.

The extent of the microbial community can also be accounted for by using a quantitative PCR as described in Wang 2010. In their studies, they were able to document every variant of the *alkB* gene in seawater surrounding Xiamen Island.<sup>24</sup> The rigor of their method is applicable to any oceanic location, and could be useful to characterize the microbiota present as well as their ability to degrade hydrocarbons.

It is well documented that salinity and temperature have a profound impact on biodegradation.<sup>9,21</sup> The extent of these factors on dilbit biodegradation can also be tested in future experiments, as to mimic seawater conditions in different settings, (i.e, an arctic spill compared to a tropical spill).

## **Conclusions**

Two biodegradation methodologies were tested for diluted bitumen. The results from the sand microcosm show minimal biodegradation but highlighted the effects of dilbit adsorption to sediment. The WAF microcosm showed noticeable losses of alkanes and PAH molecules. The aforementioned improvements can be made to the WAF microcosms to encompass more variables into oil biodegradation, and studies that involve different water sources can be utilized to incorporate their respective native flora. Overall, the method development of dilbit biodegradation experiments described in this paper serves as a framework for future studies. Using this method, the scientific community can strive to close the knowledge gap on the processes affecting this unconventional source of crude.



## References

- (1) Polaris. A Comparison of the Properties of Diluted Bitumen Crudes with Other Oils. *POLARIS Appl. Sci. Inc.* **2013**, 1–26.
- (2) National Academy of Sciences, Engineering, and Medicine. *Spills of Diluted Bitumen from Pipelines: A Comparative Study of Environmental Fate, Effects, and Response*; National Academy of Sciences, Engineering, and Medicine: Washington, DC, 2016. <https://doi.org/10.17226/21834>.
- (3) Venosa, A. D.; Suidan, M. T.; King, D.; Wrenn, B. A. Use of Hopane as a Conservative Biomarker for Monitoring the Bioremediation Effectiveness of Crude Oil Contaminating a Sandy Beach. *J. Ind. Microbiol. Biotechnol.* **1997**, *18* (2–3), 131–139. <https://doi.org/10.1038/sj.jim.2900304>.
- (4) Swarthout, R.; Nelson, R.; Hamilton, S.; Aeppli, C.; Valentine, D.; Reddy, C. *No Title*; New Orleans, 2016.
- (5) Nimana, B.; Verma, A.; Di Lullo, G.; Rahman, M. M.; Canter, C. E.; Olateju, B.; Zhang, H.; Kumar, A. Life Cycle Analysis of Bitumen Transportation to Refineries by Rail and Pipeline. *Environ. Sci. Technol.* **2017**, *51* (1), 680–691. <https://doi.org/10.1021/acs.est.6b02889>.
- (6) EPA. Enbridge Clean Water Act Settlement <https://www.epa.gov/enforcement/enbridge-clean-water-act-settlement>.
- (7) Frittelli, J.; Andrews, A.; Parfomak, P. W.; Pirog, R.; Ramseur, J. L.; Ratner, M. U.S. Rail Transportation of Crude Oil: Background and Issues for Congress Specialist in Transportation Policy Specialist in Energy Policy Specialist in Energy and Infrastructure Policy Specialist in Energy Economics Specialist in Environmental Policy. *Congr. Res. Serv.* **2014**.
- (8) CBC News. Oil pooling at creek near Gogama train derailment: Environment Ministry <https://www.cbc.ca/news/canada/sudbury/oil-pooling-at-creek-near-gogama-train-derailment-environment-ministry-1.2959886> (accessed Jun 4, 2019).
- (9) Stout, S.; Wang, Z. *Standard Handbook Oil Spill Environmental Forensics: Fingerprinting and Source Identification*; 2016.
- (10) Stringari, C. E.; Marques, W. C.; Eidt, R. T.; Mello, L. F. Modeling an Oil Spill along the Southern Brazilian Shelf: Forcing Characterization and Its Influence on the Oil Fate. *Int. J. Geosci.* **2013**, *04* (02), 397–407. <https://doi.org/10.4236/ijg.2013.42038>.
- (11) Environment Canada. *Properties, Composition and Marine Spill Behavior, Fate and Transport of Two Diluted Bitumen Products from the Canadian Oil Sands*; 2013.
- (12) Stiver, W.; Mackay, D. Evaporation Rate of Spills of Hydrocarbons and Petroleum Mixtures. *Environ. Sci. Technol.* **1984**, *18* (11), 834–840. <https://doi.org/10.1021/es00129a006>.
- (13) Gros, J.; Nabi, D.; Würz, B.; Wick, L. Y.; Brussaard, C. P. D.; Huisman, J.; Van Der Meer, J. R.; Reddy, C. M.; Arey, J. S. First Day of an Oil Spill on the Open Sea: Early Mass Transfers of Hydrocarbons to Air and Water. *Environ. Sci. Technol.* **2014**, *48* (16), 9400–9411. <https://doi.org/10.1021/es502437e>.
- (14) Bostic, J. T.; Aeppli, C.; Swarthout, R. F.; Reddy, C. M.; Ziolkowski, L. A. Ongoing Biodegradation of

- Deepwater Horizon Oil in Beach Sands: Insights from Tracing Petroleum Carbon into Microbial Biomass. *Mar. Pollut. Bull.* **2018**, *126* (March 2017), 130–136.  
<https://doi.org/10.1016/j.marpolbul.2017.10.058>.
- (15) Mcconkey, B. J.; Hewitt, M. L. Natural Sunlight Induced Photooxidation of Naphthalene in Aqueous Solution. *Water Air Soil Pollut.* **2002**, No. October 2002, 193–194.  
<https://doi.org/10.1023>.
  - (16) Atlas, R. M. Microbial Degradation of Petroleum Hydrocarbons : An Environmental Perspective. *Microbiol. Rev.* **1981**, *45* (1), 180–209.
  - (17) Prince, R. C.; Owens, E. H.; Sergy, G. A. Weathering of an Arctic Oil Spill over 20 Years: The BIOS Experiment Revisited. *Mar. Pollut. Bull.* **2002**, *44* (11), 1236–1242.  
[https://doi.org/10.1016/S0025-326X\(02\)00214-X](https://doi.org/10.1016/S0025-326X(02)00214-X).
  - (18) Olajire AA, E. J. Aerobic Degradation of Petroleum Components by Microbial Consortia. *J. Pet. Environ. Biotechnol.* **2014**, *05* (05). <https://doi.org/10.4172/2157-7463.1000195>.
  - (19) Prince, R. C. *Handbook of Hydrocarbon and Lipid Microbiology*; 2010.  
<https://doi.org/10.1007/978-3-540-77587-4>.
  - (20) Holden, P. A.; Hersman, L. E.; Firestone, M. K. Water Content Mediated Microaerophilic Toluene Biodegradation in Arid Vadose Zone Materials. *Microb. Ecol.* **2001**, *42* (3), 256–266.  
<https://doi.org/10.1007/s00248-001-0010-3>.
  - (21) Sharma, P.; Schiewer, S. Assessment of Crude Oil Biodegradation in Arctic Seashore Sediments: Effects of Temperature, Salinity, and Crude Oil Concentration. *Environ. Sci. Pollut. Res.* **2016**, *23* (15), 14881–14888. <https://doi.org/10.1007/s11356-016-6601-9>.
  - (22) Word, J. Environmental Impacts of Arctic Oil Spills and Arctic Spill Response Technologies. *Arct. Oil Spill Response Technol. Jt. Ind. Programme* **2014**.
  - (23) Blumer, M.; Sass, J. Oil Pollution: Persistence and Degradation of Spilled Fuel Oil. *Science* (80-. ). **1972**, *176* (4039), 1120–1122. <https://doi.org/10.1126/science.176.4039.1120>.
  - (24) Wang, L.; Shao, Z. Diversity and Abundance of Oil-Degrading Bacteria and Alkane Hydroxylase (AlkB) Genes in the Subtropical Seawater of Xiamen Island. *Microb. Ecol.* **2010**.  
<https://doi.org/10.1007/s00248-010-9724-4>.
  - (25) Shrestha, P.; Meisterjahn, B.; Klein, M.; Mayer, P.; Birch, H.; Hughes, C. B.; Hennecke, D. Biodegradation of Volatile Chemicals in Soil: Separating Volatilization and Degradation in an Improved Test Setup (OECD 307). *Environ. Sci. Technol.* **2019**, *53* (1), 20–28.  
<https://doi.org/10.1021/acs.est.8b05079>.